

DYNAMIC FRACTURE TOUGHNESS OF POLYMER COMPOSITES

A Thesis

by

HARMEET KAUR

Submitted to the Office of Graduate Studies of
Texas A&M University
in partial fulfillment of the requirements for the degree of

MASTER OF SCIENCE

December 2010

Major Subject: Mechanical Engineering

DYNAMIC FRACTURE TOUGHNESS
OF POLYMER COMPOSITES

A Thesis

by

HARMEET KAUR

Submitted to the Office of Graduate Studies of
Texas A&M University
in partial fulfillment of the requirements for the degree of

MASTER OF SCIENCE

Approved by:

Chair of Committee,	Jyhwen Wang
Committee Members,	Anastasia Muliana
	Alex Fang
Head of Department,	Dennis L. O'Neal

December 2010

Major Subject: Mechanical Engineering

ABSTRACT

Dynamic Fracture Toughness
of Polymer Composites. (December 2010)
Harmeet Kaur, B.E., Rajasthan University, India
Chair of Advisory Committee: Dr.Jyhwen Wang

Polymer composites are engineered materials widely being used and yet not completely understood for their dynamic response. It is important to fully characterize material properties before using them for applications in critical industries, like that of defense or transport. In this project, the focus is on determining dynamic fracture toughness property of fiber reinforced polymer composites by using a combined numerical- experimental methodology. Impact tests are conducted on Split-Hopkinson pressure bar with required instrumentation to obtain load-history and initiation of crack propagation parameters followed by finite element analysis to determine desired dynamic properties. Single edge notch bend (SENB) type geometry is used for Mode-I fracture testing and similarly end-notched flexure (ENF) type of geometry is proposed to test the samples for Mode-II type of fracture. Two different linear elastic fracture mechanics approaches are used- crack opening displacement and strain energy release rates. Dynamic fracture toughness values of around $50 \text{ MPa}\sqrt{m}$ and $100 \text{ MPa}\sqrt{m}$ in Mode-I, whereas, around $40 \text{ MPa}\sqrt{m}$ and $6 \text{ MPa}\sqrt{m}$ in Mode-II are observed for carbon-epoxy and fiberglass-epoxy composites respectively. To provide a better estimate of material response, Hashin damage model is employed which takes into account non-linear behavior of composites. As observed in previous studies, values estimated using a non-linear response of composite laminates are nearly three times as high, therefore, using a linear elastic material model could underestimate a material's capacity to sustain dynamic loads without failure. It is concluded

that fracture initiation toughness property is rate dependent and is higher when subjected to dynamic loads. Microscopic examination of damaged samples and a higher value of dynamic fracture toughness for fiberglass-epoxy laminates as compared to carbon-epoxy laminates suggest that dynamic fracture toughness is also a function of many other variables like mode of fracture, dominant damage criteria, manufacturing process, constituent materials and their ratios.

To My Family and Friends

ACKNOWLEDGMENTS

I take this opportunity to express my deepest gratitude to Dr. Jyhwen Wang, my advisor, for all the support and guidance he has given me throughout my graduate study and thesis work. His suggestions and constant encouragement helped me a lot.

I appreciate the opportunity given to me by Dr. Carlos Rubio and the immense support provided by his team at CIDESI Mexico, especially Mr. Jesus Martinez and Mr. Christian Felix Martinez for their help in completing experimental work. I would also like to thank Mr. Rohit Agarwal at Augusta Fiberglass for extending his help in providing us samples for this project.

I am grateful to my committee members, Dr. Alex Fang and Dr. Anastasia Muliana who have been helpful and generous with their time and expertise to evaluate my thesis.

I am grateful to my family and friends, for the tremendous amount of inspiration and moral support they have given me.

TABLE OF CONTENTS

CHAPTER		Page
I	INTRODUCTION	1
II	BACKGROUND AND LITERATURE REVIEW	5
	A. Fracture toughness	5
	B. Dynamic fracture initiation toughness	7
	C. Composite dynamic fracture	8
	D. Fracture toughness tests	10
	E. Damage model	12
III	DESCRIPTION OF METHODOLOGY	14
	A. Sample and specimen description	14
	B. Experiments	17
	1. Quasi-static tests	18
	2. Impact tests	19
	C. Description of methods to obtain dynamic fracture toughness	22
	1. Crack opening displacement method	24
	2. Strain energy release rate method	25
	D. Finite element analysis	27
	1. COD and ERR calculation based on LEFM	28
	2. COD and ERR calculation based on damage model . .	29
IV	EXPERIMENTAL RESULTS	31
	A. Quasi-static test results	31
	1. Mode-I quasi-static test	31
	2. Mode-II quasi-static test	31
	B. Impact tests	33
	1. Mode-I impact test	38
	2. Mode-II impact test	38
V	FRACTURE TOUGHNESS CALCULATIONS	43
	A. Quasi-static fracture toughness	43
	1. Mode-I fracture toughness	44
	2. Mode-II fracture toughness	46

CHAPTER	Page
B. Dynamic fracture initiation toughness	46
1. Mode-I dynamic fracture toughness	47
2. Mode-II dynamic fracture toughness	53
VI RESULTS AND DISCUSSIONS	56
A. Discussion on quasi-static fracture toughness results	56
B. Discussion on dynamic fracture initiation toughness	59
VII CONCLUSIONS	70
REFERENCES	73
APPENDIX A	77
APPENDIX B	82
VITA	87

LIST OF TABLES

TABLE		Page
I	Material elastic constants	27
II	Maximum load endured P_{max} and Peak loads P_Q at fracture initiation for different composite laminates and modes of fracture	33
III	Wave speeds and traveling times making a particular angle to laminate fiber direction	37
IV	Mode-I quasi-static fracture toughness values (K_{IC})	45
V	Mode-II quasi-static fracture toughness values (K_{IIC})	46
VI	Mode-I dynamic fracture toughness values (K_{ID})	52
VII	Mode-II dynamic fracture toughness values (K_{IID})	53

LIST OF FIGURES

FIGURE		Page
1	Effect on modulus due to addition of fibers to matrix	2
2	Fracture toughness vs thickness of sample [1]	6
3	Loading configuration of three point bend set-up developed by Yokoyama[2]	11
4	Steps involved in achieving the objective of this project	15
5	Laminate prepared from prepregs	17
6	Specimen geometries for experiments (All dims in mm.)	18
7	Three-dimensional representation of Mode-I samples in test set-up . .	19
8	SENB sample mounting for impact tests	21
9	Picture showing position of strain gauge bonded very near to crack-tip	21
10	Sample of wave signal output from strain gauges attached to SHPB set-up	22
11	Load vs displacement plot of SENB sample under quasi-static loading	32
12	Load vs displacement plot of ENF sample under quasi-static loading	34
13	Strain pulses as obtained in impact testing	35
14	Crack tip strain gauge pulse showing time of initiation of crack . . .	37
15	Load vs time plot of various PMCs for Mode-I impact tests	39
16	Pictures of impact damaged carbon-epoxy laminate specimen	40
17	Impact damaged fiberglass-epoxy laminate	41

FIGURE	Page
18	Strain gauge signals recorded for Mode-II impact tests 41
19	Load vs time plot of various PMCs for Mode-II impact tests 42
20	Comparison of stress distributions observed in fiberglass-epoxy laminate tested for Mode-I quasi-static fracture toughness 44
21	Comparison of stress distributions observed in fiberglass-epoxy laminate tested for Mode-II quasi-static fracture toughness 45
22	Crack opening displacement history from impact simulation of SENB samples 48
23	Mode-I stress intensity factor vs time for carbon comparing material models 49
24	Mode-I stress intensity factor history of fiberglass and matted fiberglass assuming linear elastic material model 50
25	Mode-I energy release rate vs time for fiberglass and matted fiberglass laminates using linear elastic model 51
26	Mode-I energy release rate vs time for carbon using different material models 52
27	Mode-II energy release rate vs time for fiberglass and matted fiberglass laminates using linear elastic model 54
28	Mode-II energy release rate vs time for carbon using different material model 55
29	Microscopic pictures comparing interfacial bond characteristics of carbon-epoxy and fiberglass-epoxy samples 62
30	Pictures from microscope comparing Mode-II in carbon-epoxy and fiberglass-epoxy samples 65
31	Pictures from microscope comparing Mode-II crack initiation characteristics in carbon-epoxy and fiberglass-epoxy samples 66
32	Study of Mode-I type dynamic crack opening behavior of carbon epoxy laminate 67

FIGURE	Page
33 Study of Mode-II type dynamic crack opening behavior of carbon epoxy laminate	68

CHAPTER I

INTRODUCTION

Composite materials are receiving wide attention lately as they have many attractive mechanical properties. Being lighter for similar strength ratings and also corrosion resistant, they are considered superior to metals for certain applications. Composites are engineered materials made up of two or more constituents to form a single bulk mass. On microscopic scale, matrix and reinforcement exhibit their individual characteristic properties but on a larger scale they combine to form a composite material with superior characteristics. There are a number of options for matrix and reinforcing materials and they can be mixed in different combinations, ratios, and directions to obtain a composite material with desired properties. There are many types of composite materials like metal matrix composites, polymer composites, ceramic matrix composites etc. depending on the type of reinforcing and matrix material.

Polymer matrix composites (PMC) consist of polymer resin as matrix and fibrous reinforcing dispersed phase. Carbon, Fiberglass and Kevlar are used as reinforcing fiber material. Use of polymer resin in itself is limited due to inferior mechanical properties when compared to metals. However, they have an advantage because of their ability to be formed into complicated shapes. Materials like aramid and glass have high tensile and compressive strengths but not in their bulk forms due to the presence of random flaws causing them to fail much below their actual failure point. To overcome this drawback, these materials are drawn into fibers which will have flaws, but few of the perfect ones in a bundle will help in exhibiting almost the predicted strength characteristics. Using a bundle of fibers alone will provide good characteris-

The journal model is *IEEE Transactions on Automatic Control*.

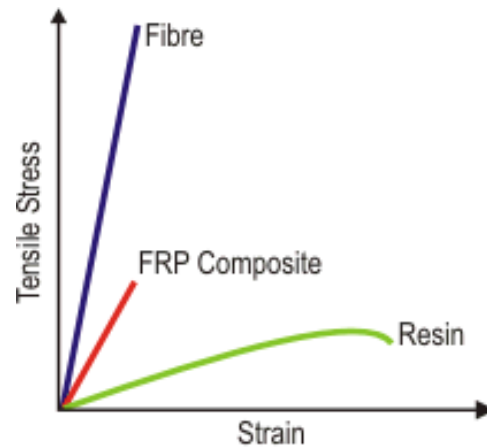


Fig. 1. Effect on modulus due to addition of fibers to matrix

tics only in the direction of fibers but when combined with a resin system exceptional properties can be obtained. Resin system spreads the load between fibers and protects the fibers against abrasion, wear and impact. Properties of resulting composite will combine the characteristics of resin system and fibers both (as shown in Fig. 1), thus exhibiting many useful properties like high tensile strength, high stiffness, high fracture toughness, good abrasion resistance, good puncture resistance, good corrosion resistance, low cost etc. The properties of PMCs can be varied, depending on functional requirements, with the change of orientation, length, type, concentration of fibers and properties of resin system.

Polymer composites can be manufactured in a number of ways but are prone to having defects like voids, cracks, inclusions like in metals. Certain applications require careful designing as the components should be safe to use in their service life. In order to produce an optimized design, it is essential to evaluate finished material for its properties. Fracture toughness is a fracture mechanics parameter that gives a measure of pre-cracked material's ability to carry load. A non-uniform material having defects cannot be estimated for its strength in impact using conventional mechanics.

The conventional theories and tests assuming a homogeneous material would over or under estimate its resistance to fracture. Von-Mises or Tresca yield strength criteria do not account for stress concentrations occurring near the defects. These stress concentrations are localized and make the material more prone to failures. Fracture mechanics parameters include the effects of concentration of stresses near crack tips. Among the various existing theories, linear elastic fracture mechanics is very basic and widely used due to its simplistic approach. It is useful in studying stable crack growth in structure, which are in a state of equilibrium. It is important to evaluate fracture toughness in quasi-static loading conditions that are easy to achieve and observe and has already been standardized.

As the loading rates are subsequently increased to duplicate real impact conditions with strain rate of more than 1000/sec, it gets difficult to observe the fracture toughness parameters and also the change in material behavior. Material may become stiffer increasing its ability to resist fracture. High loading rates may also make the material more brittle resulting in reduced ability to yield and thus low fracture toughness. Therefore, rate of loading is an important parameter when measuring fracture toughness. Composite fracture toughness measurements at high loading rates are still a challenge. It is one of the important and useful properties of polymers composites to ensure safe service life of finished products. Thus, it is an important area of research to develop methods for determining dynamic fracture toughness. For example: Kevlar composites are used for bullet proofing and are required to be highly impact resistant. Various other applications and types may be required to be impact resistant even though it is not their primary function.

A lot of research work has been published in material dynamic fracture toughness characterization but still an improvement can be made in methods to determine dynamic fracture toughness property of a composite material. This project will con-

tribute by describing a combined experimental-numerical approach to determine the dynamic fracture initiation toughness of polymer composites at high strain rates. Dynamic fracture tests are conducted on three-point bend samples of carbon and fiberglass laminates on Split Hopkinson pressure bar set-up and numerical simulation are conducted to evaluate stress intensity factors as a function of time. Dynamic fracture initiation toughness is the stress intensity factor value at initiation of crack propagation.

CHAPTER II

BACKGROUND AND LITERATURE REVIEW

A. Fracture toughness

Linear elastic fracture mechanics is simple and basic approach to evaluate fracture toughness property of a material. This theory assumes an isotropic brittle material behavior. Thus, no yielding is predicted near the crack tip zone. The stresses are calculated using theory of elasticity and are given as follows:

$$K_I = k\sigma\sqrt{\pi a} \quad (2.1)$$

where,

K_I is the fracture toughness

σ is the applied stress

a is the crack length

k is a dimensionless parameter related to crack length and geometry

Crack grows when stresses near the crack tip exceed fracture toughness of the material. Therefore, it is essential to determine the fracture toughness property of a material as components are prone to presence of cracks and risk failure. Quasi-static fracture toughness measurement procedures have been standardized by ASTM E399 for plane stress and plane strain conditions. Plane strain fracture toughness gives the true material property (K_{IC}). It gives the highest value of stress occurring near the crack tip before the material fails but only under a particular condition of plane strain. Plane stress condition using a specimen with negligible thickness will give the highest possible fracture toughness value for that material. Therefore, fracture toughness is highly dependent on the thickness of material sample tested as shown in

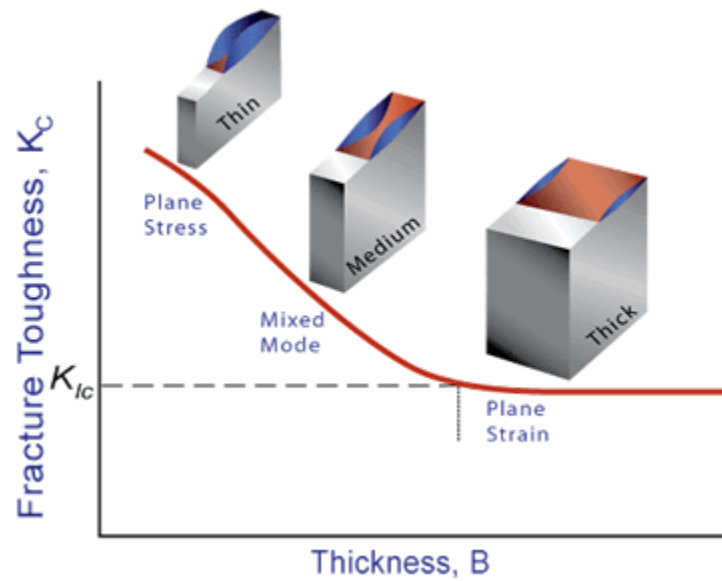


Fig. 2. Fracture toughness vs thickness of sample [1]

Fig. 2.

The procedure followed in this project assumes plane stress conditions for simplicity. According to classical laminate theory, uni-directional continuous fiber composites exhibit orthotropic symmetry and there are nine independent elastic constants for an orthotropic material.

$E_1, E_2, E_3, G_{12}, G_{23}, G_{31}, \nu_{12}, \nu_{13}$ and ν_{23}

Assuming plane stress conditions for dynamic tests, the elastic constants are reduced to just five $E_1, E_2, G_{12}, \nu_{12}$, and ν_{23} as explained below[3].

$$E_2 = E_3$$

$$G_{31} = G_{12}$$

$$\nu_{12} = \nu_{13}$$

$$G_{23} = E_2 / (2(1 + \nu_{23}))$$

B. Dynamic fracture initiation toughness

Fracture toughness is a rate dependent parameter. This value may increase or decrease with an increase in strain rates depending on material's response. It is important to determine fracture toughness property of the material for a component at loading conditions as per its desired service life. There are two categories of dynamic fracture mechanics. First is related to situation when the crack reaches instability and starts propagating rapidly in the material mass. The second concerns a stationary crack in the material subjected to impact forces. This problem involves an interesting study of crack propagation initiation properties of material [4]. It should be independent of the geometry of sample used for testing. If the whole component is observed until failure i.e. a crack is allowed to propagate through the entire cross-section then resulting property will be fracture toughness of that particular part depending on its design and geometry.

Dynamic fracture material behavior has been evaluated using a number of combined numerical-experimental approaches. Dynamic loads were measured accurately in experiments done on wedge loaded or circumferentially notched bar samples. But the dynamic fracture initiation toughness was obtained using conventional static re-

lations. Photo elastic methods were developed to measure directly the dynamic fracture initiation toughness but it requires an expensive instrumentation. Method by Yokoyama [5] allowed complete dynamic analysis but required a long computing time posing difficulty in coping with experimental data. An attempt to provide a simpler approach for measuring the dynamic fracture toughness property of materials was put forth by proposing a dynamic relation for stress intensity factor [6]. However, the available methods are not enough to accurately observe the material response at every time instant. Therefore, it is still a challenge to get true value of dynamic fracture initiation toughness of composites. Several interesting attempts are briefed as follows.

Rubio et al. [7] studied the dynamic fracture toughness of pre-fatigued aluminum and steel samples impacted with different projectile velocities. SHPB experimental set-up was used by them, for three-point bend type geometry, to obtain the load-history and time at fracture. LS-DYNA solver was then used to obtain displacements very near the crack-tip. Crack opening displacement (COD) was used to find the stress intensity factor history and stress intensity factor at the time of initiation of crack propagation is the dynamic fracture initiation toughness.

Fengchun et al. [6] again used SHPB for impact testing of pre fatigued high strength steel specimen. They used simple static formulae to calculate stress intensity factor under dynamic conditions. The values obtained are compared with FEM analysis to ensure reliability.

C. Composite dynamic fracture

Composites due to their heterogeneities are difficult to model and thus have not been studied extensively for their dynamic response. Moreover, they have inherent flaws

like voids and cracks that degrade properties like stiffness, strength on applying loads and they also behave differently depending on ply arrangement and strain rates [8]. Composite in quasi-static or static loading conditions have been studied and also standardized in ASTM E1922. For strain rates above 1000/s the non-linearity of the stress-strain curves reduces. Due to its viscoelastic nature, the material also acts stiffer as the strain rates are increased. Most of the results of dynamic tests show a higher value of fracture toughness than the quasi-static values like a difference of 1.3 suggested by Tsai and Sun [9] using SHPB in compression. They also showed that depending on strain rates, maximum normal stress is 50-100% higher for dynamic conditions than quasi-static conditions. One of their important observation was, even though both matrix and fiber are sensitive to strain rates, fibers dominate in influencing the properties of the composite.

Intralaminar crack propagation studied in this project is difficult to simulate as accumulation of damage and hence crack propagation can occur in an unpredictable path or manner. Camanho [10] described interlaminar and intralaminar/translaminar type of cracking observed in composites and also different models used to simulate the material response. Camanho also claimed that intralaminar damage occurs at different orientation depending on ply thickness and arrangement. Dynamic interlaminar mode is widely studied using Teflon and Aluminum inserts as flaws between laminate plies [11], [12], [13]. Sun et al. [12] used SHPB tests to measure dynamic delamination toughness of carbon and fiberglass polymer composites. Teflon inserts were used and loaded by a wedge to obtain Mode-I type of crack opening. Two crack propagation gauges were used having ten parallel resistors to obtain crack traveling speed. SHPB tests were conducted for dynamic loading history output and used as FEA boundary condition to evaluate the dynamic fracture initiation toughness as well as the dynamic fracture toughness. Modified crack closure technique was used to

get the strain energy release rates. Finally, stress intensity factor was found from the strain energy release rate output using a corrected equation to include the dynamic effects.

D. Fracture toughness tests

Charpy tests - conventional or instrumented, are used to determine total energy dissipated in a fracture event but it is difficult to understand the inertial effects involved in fracture process and plane strain conditions are not achieved. Strain gauge attached to impacting hammer of the machine can give the loading history required for calculating dynamic parameters. But the measured values are overestimated due to inertia and oscillation of the sample. Also, it is not possible to accurately determine the initiation time of crack propagation. Charpy impact test conditions are limited by lower strain rates. Improvements in achieving plane strain conditions for accurate fracture toughness determination came in the form of Drop weight test technique. This technique used a large sample allowing a plane strain analysis. Further improvement was made by measuring load from the stress waves in the elastic bar used for drop weight testing.

To overcome above drawbacks of conventional dynamic tests, SHPB was introduced for measuring fracture toughness at very high strain rates. It closely simulates real world dynamic loading condition a material may have to withstand during its service life. Split Hopkinson bar technique was originally implemented for determining elastic wave properties of materials. It was later modified to study the dynamic effects under tension, compression, bending by using one dimensional stress-wave theory by Davies [14] and Kolsky [15]. SHPB was first used for fracture measurements in 1970s by Costin et al. [16]. Several configurations are possible in SHPB set-up

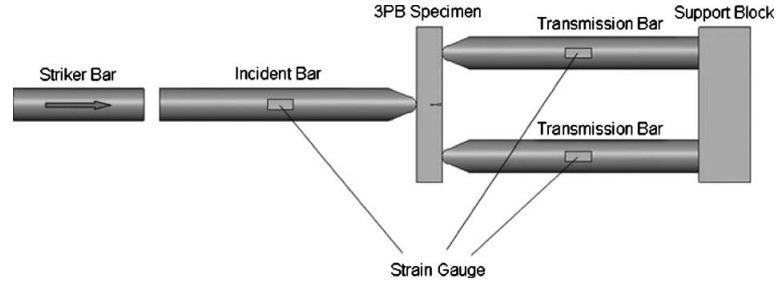


Fig. 3. Loading configuration of three point bend set-up developed by Yokoyama[2] for studying different modes. Three-point bend configuration devised by Yokoyama, as shown in Fig. 3, was later proposed to evaluate dynamic fracture toughness by simple transverse wave propagation analysis [5]. The novel three point bend configuration uses one incident bar and two transmitter/supporting bars. Few important conclusions of the studies done by Yokoyama and Kishida are: loss of contact between the impacting bar and sample, peak point on the loading plot does not indicate the instance of crack initiation, quasi-static equilibrium conditions are not achieved in this set-up and thus different results are obtained for quasi-static and dynamic tests. The equations developed by Kolsky for finding incident $P_i(t)$ and transmitted $P_t(t)$ loads are as follows:

$$P_i(t) = EA[\epsilon_i(t) + \epsilon_r(t)] \quad (2.2)$$

$$P_t(t) = EA\epsilon_t(t) \quad (2.3)$$

where,

E and A are Young's modulus and cross-sectional area respectively of the bars

$\epsilon_i(t)$ is the incident compressive stress as measured by the strain gauge coincident bar

$\epsilon_r(t)$ is the reflected tensile pulse in the incident bar

E. Damage model

Material's resistance to fracture is governed by yielding at the crack tip that absorbs a large fraction of fracture energy. Most of the fiber reinforced composites have little capacity to yield plastically. Yielding in composites is dominated by formation of damage zone having sub critical cracks in different directions. The size of this damage zone greatly affects the fracture toughness of the composite, large size allowing more absorption of energy and thus larger fracture toughness. The extension of damage zone is closely related with the LEFM parameter K_I . Mendell et al. [17] described the characteristics of damage zone as, elastic yielding of pre-cracked composite on applying load. Subsequent formation of sub-critical cracks is governed by local crack tip stresses leading to crack extension or delamination on reaching threshold value of stresses.

It is possible to model failure of a pre-cracked laminate using fracture mechanics approach as well as damage mechanics approach. Fracture mechanics approach seems to be appropriate for parts with pre-existing cracks. Linear elastic fracture (LEFM) does not account for changes in mechanical behavior of materials and their subsequent stress redistribution in the structure induced by accumulated process of material degradation, particularly near the crack tip. Few studies [18], [19] have effectively used damage model to investigate crack propagation considering crack as a set of points for which damage has reached its critical value. Damage variable used in continuum damage mechanics is based on the effective stress concept; it represents an average material degradation reflecting various types of microscopic defects at different damage states of the material. Therefore, crack will propagate when accumulation of damage reaches a critical value for that material. As done in previous studies, material behavior at onset of cracking can be determined using damage

mechanics approach applied to a macro crack.

Various models (such as that of Hashin, Tsai-Wu) have been developed to describe composite material behavior. These models are also suitable for high strain rate studies. Some such models are now implemented in softwares like ABAQUS and ANSYS, while some others are used by introducing user defined material subroutines. Modified Hashin damage model has been implemented in ABAQUS and also used to study fracture of a composite with blunt notch by Lapczyk and Hurtado [20].

CHAPTER III

DESCRIPTION OF METHODOLOGY

This project develops methodologies for determining dynamic fracture toughness of composite materials and also the instant of crack opening in a laminate composite impacted at high strain rates. Steps to be followed are:

- Impact testing in Mode-I and Mode-II using split Hopkinson pressure bar apparatus
- Finite element (ABAQUS) dynamic analysis to obtain crack opening displacement and energy release rate
- Determining dynamic fracture toughness from empirical relations using experimental data and finite element analysis

This research will also compare dynamic fracture toughness obtained from two different approaches in finite element analysis:

1. Linear elastic fracture mechanics model
2. Damage model

Sequential steps followed in the project are shown in Fig. 4

A. Sample and specimen description

Composites are used in heavy industrial applications like that of aerospace, pressure vessels and transportation. Complex composite structures require careful methods of mechanical and adhesive joining but these methods also increase the number of possible defect sites. As certain industries require precise control and involve critical

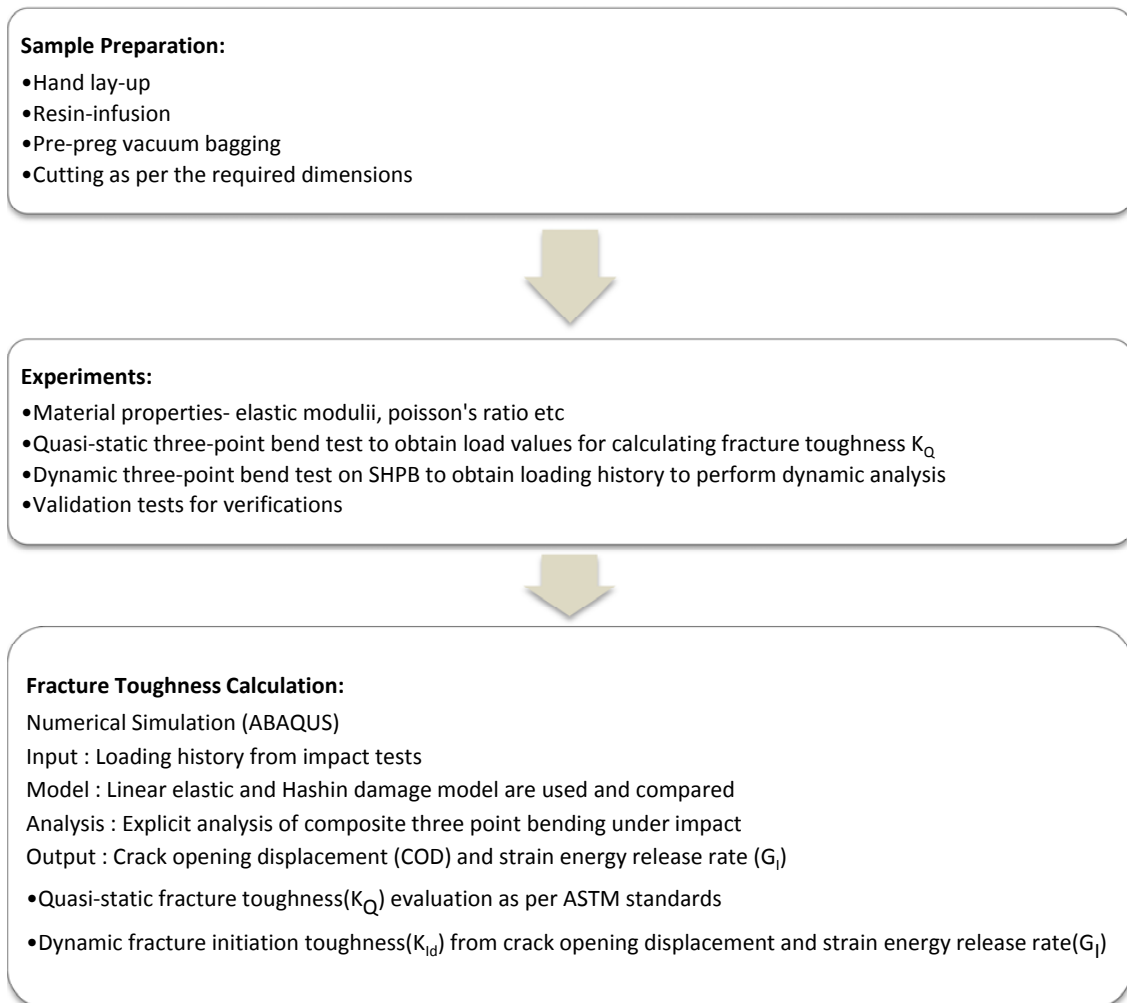


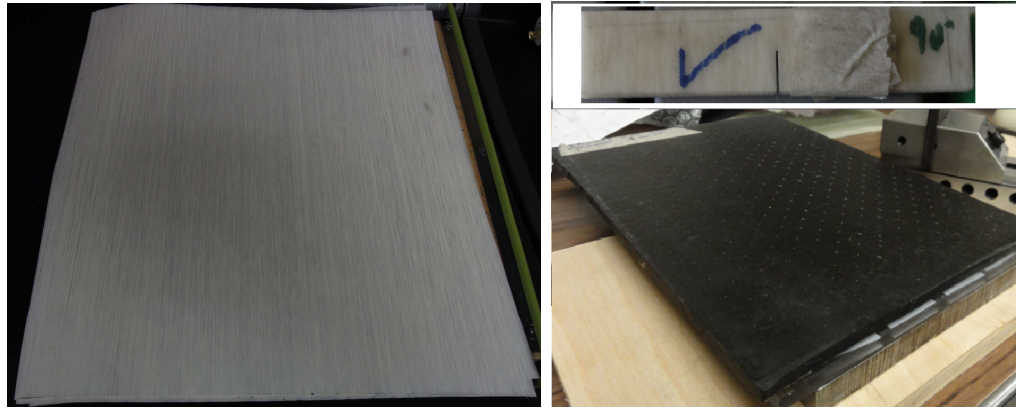
Fig. 4. Steps involved in achieving the objective of this project

applications, they devise optimized composite manufacturing method suiting their requirements. There are a number of ways to prepare composite materials and yet no universal standards have been put forth to guide the composite preparation procedure. Various manufacturing methods can be listed as follows[21]:

- Compression Molding
- Filament Winding
- Pultrusion
- Injection Molding
- Autoclave Technique
- Diaphragm Forming Processes

Fracture toughness being a material property should preferably be measured for material with homogeneous and consistent properties. Thus, in this project, specimens were initially produced from resin infusion process at the Nonmetallic Material Laboratory in the Department of Engineering Technology and Industrial Distribution. To obtain more consistent samples with possibly lesser voids, samples made from carbon fiber preregs were provided by a research collaborator at Centro de Ingeniera y Desarrollo Industrial (CIDESI), Mexico. Picture of fiberglass prepreg used by CIDESI for their experiment can be seen in Fig. 5. Both these processes come under the category of compression molding methods. Also, to compare properties of two types of polymer composites, fiberglass laminates made by traditional hand lay-up method were shared by AUGUSTA Fiberglass.

Composite plates are cut to required dimension of single edge notch bend (SENB) and end notched flexure (ENF) geometry using a diamond cutter as given in Fig. 6. Since metal bond diamond wheel of 0.43mm thickness is used, it can cut approximately a 0.50mm notch in the sample for fracture toughness testing.



(a) Fiberglass prepreg

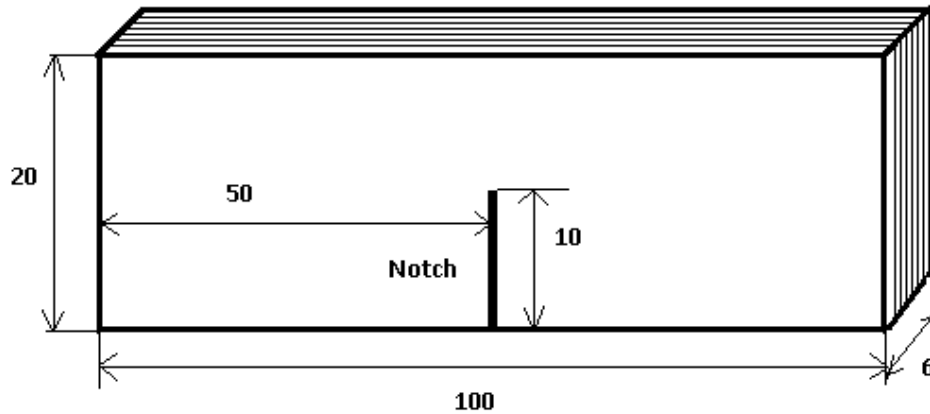
(b) Fiberglass laminate cut sample and carbon laminate prepared by laying and curing prepregs

Fig. 5. Laminate prepared from prepregs

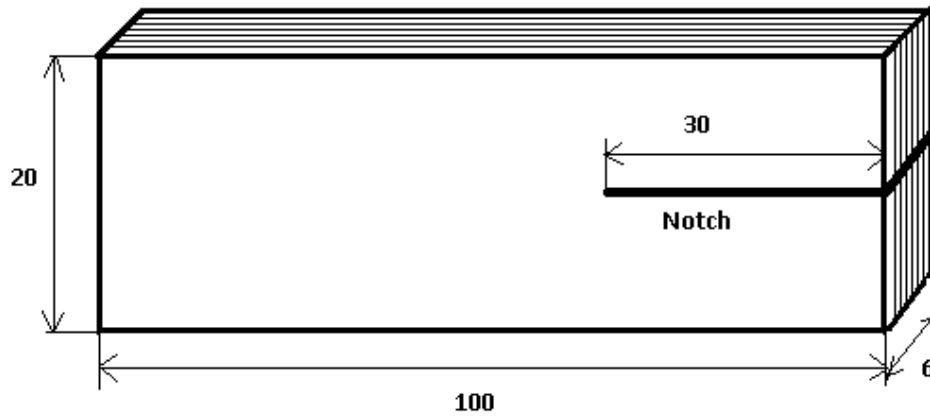
Most of the studies performed earlier were to measure the delamination fracture toughness. To further study material behavior in other types of failure modes, a notch is cut across plies as shown in Fig. 7.

B. Experiments

There is no defined method to determine dynamic fracture initiation toughness of a material when measured at very high strain rates of the order of 1000/sec. Special techniques are required to estimate properties for material under impact conditions. Combined numerical-experimental approach described in this project, required series of experiments and numerical simulations to obtain desired results and a basis for comparison. Below is a brief description of conducted experiments.



(a) SENB specimen with 0.5mm thick center notch



(b) End notched flexure specimen with 0.5mm thick notch

Fig. 6. Specimen geometries for experiments (All dims in mm.)

1. Quasi-static tests

Quasi-static fracture tests can be conducted on MTS 810 machine using a three point bend fixture. The tests are performed at very low loading rates of around 0.10 mm/min as recommended by ASTM to ensure quasi-static test conditions. The testing machine's load and displacement sensors give the load, extension, stresses and strains, at each time instant, as output. Fracture toughness K_{IC} is calculated from formula used in ASTM E399 for SENB specimens and is given in Equ.(3.1).

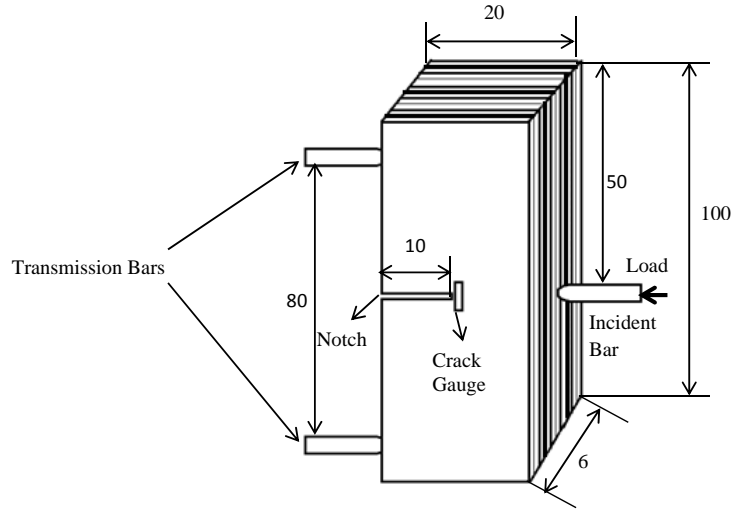


Fig. 7. Three-dimensional representation of Mode-I samples in test set-up

$$K_{IQ} = (P_Q S) / (BW^{3/2}) f(a/W) \quad (3.1)$$

where

$$f(a/W) = \frac{3\sqrt{\frac{a}{W}}}{2(1 + 2\frac{a}{w})(1 - \frac{a}{W})^{3/2}} \left[1.99 - \frac{a}{W} \left(1 - \frac{a}{W} \right) \left(2.15 - 3.93\frac{a}{W} + 2.7\left(\frac{a}{W}\right)^2 \right) \right]$$

K_{IQ} is the tentative Mode-I fracture toughness and P_Q is peak applied load at fracture initiation. P_Q is determined by an intercept of 95% offset of slope of linear portion in load-displacement curve. Tests are conducted for both Mode-I and Mode-II using the same specimen dimensions as given in Fig. 6. Finite element analysis directly provides critical strain energy release rate G_{IIC} to give dynamic fracture toughness property K_{IIC} .

2. Impact tests

Impact tests can be conducted in a number of ways depending on the output desired, geometry used, and range of operation. For this project on dynamic fracture

toughness, SHPB set-up is chosen to approach conditions of very high strain rates. One incident bar and two transmitter bars are required for a three-point bend configuration. The specimen rests on a support with bar tips just touching its surface. Each bar has a strain gauge that detects strain waves traveling, in the form of voltage pulses. An additional strain gauge(SG) is required near the crack tip to detect signals just at the instant of crack propagation. SG signals are very weak to be recorded by an oscilloscope, therefore, each signal is amplified by an amplifier before supplying to oscilloscope as input. But, the set-up can be modified to suit output required from the experiment. The apparatus consists mainly of an air gun, a striker bar, three Hopkinson pressure bars (one incident and two transmitters), a velocity measuring device and recording equipment. The pressure bars (1800 mm long) and the striker bar (152.4 mm long) were made of 19 mm diameter high strength steel (Maraging C300). The pre cracked composite bend specimen was placed between the incident and two transmitter bars as shown in Fig. 8.

Impact of striker bar into the face of incident bar develops a longitudinal compressive pulse $\epsilon_i(t)$ that is propagated along this bar. Part of the compressive incident pulse $\epsilon_i(t)$ is transmitted through the specimen, causing its fracture and into transmitter bars as compressive pulse $\epsilon_t(t)$, while part of which is reflected back to the incident bar as a tensile pulse $-\epsilon_r(t)$. The incident load $P_i(t)$ and the transmitted load $P_t(t)$ are then determined from one-dimensional theory of elastic wave propagation as explained in Equ.(2.2). The zero reference of loading history is obtained by shifting wave signals on the time axis to the instant when incident wave just arrives at uncracked mid length surface of bend sample.

The three strain gauges having a gauge length of 1.6mm are VISHAY CEA 06 062 UW 120. Strain gauge on incident bar is placed 900mm from the impact end and strain gauges on the transmitter bar are placed at 900mm from the specimen.

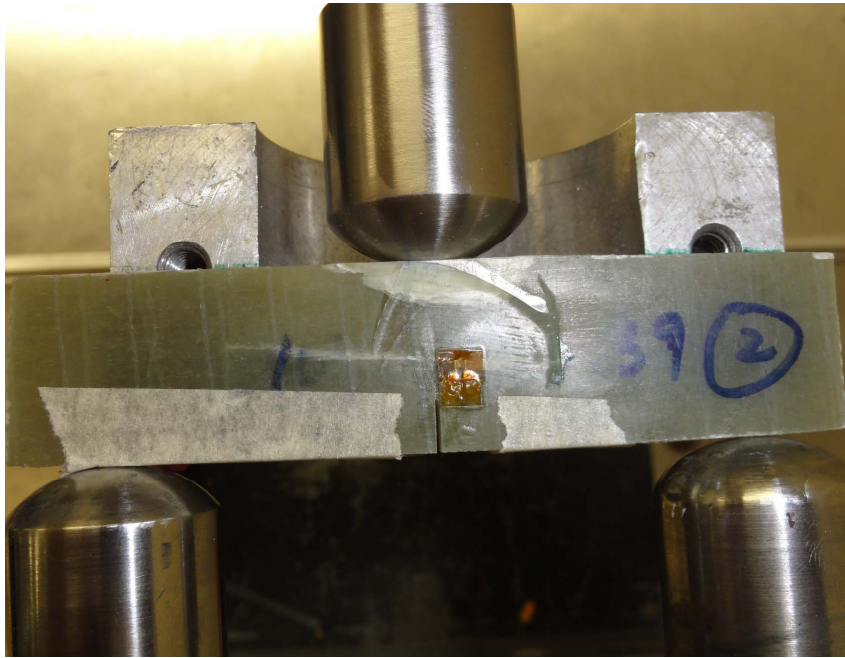


Fig. 8. SENB sample mounting for impact tests

The strain gauge (VISHAY CEA 13 032 UW 120) 1mm to 2mm from sample crack-tip is mounted as shown in Fig. 9. All the strain gauges used in this set-up are bonded using M Bond 200 adhesive. The signals from strain gauges are conditioned by amplifier VISHAY 2311 and these inputs are given to the three input channels of oscilloscope for recording the impact event. A typical signal obtained from this dynamic experiment is as shown in Fig. 10.



Fig. 9. Picture showing position of strain gauge bonded very near to crack-tip



Fig. 10. Sample of wave signal output from strain gauges attached to SHPB set-up

C. Description of methods to obtain dynamic fracture toughness

There are many methods to measure quasi-static fracture toughness of a material. Available fracture toughness relations are for a material under loading conditions that maintain equilibrium during complete event of loading. In a dynamic case it is noted that inertial effects, vibration, stress waves and acceleration of specimen come into play and stress intensity values show a marked difference compared to its quasi-static values.

Dynamic events are difficult to monitor and hence J-integral and crack tip opening displacement methods are used in this exercise to determine the fracture toughness property of a material. Non-linear finite element analysis is performed to obtain the parameters which are then used in static relations to calculate stress intensity factor varying with time.

Following are common fracture toughness parameters:

- **Stress intensity factor(K)**: It is a stress based parameter that depends on applied load at fracture and material geometry.
- **Crack opening displacement(COD)**: This approach has been developed mainly in UK with a chief purpose of studying welds and welded structural steel components that are difficult to simulate. Crack opening displacement (COD) at the original crack tip is called crack-tip opening displacement (CTOD). An initially sharp crack blunts by plastic deformation at the original tip, therefore, a purely elastic material will have no CTOD. It is a strain based criteria that depends on material characteristics, elastic or plastic. It is expected that every material has a critical CTOD that can be used as a fracture criterion.
- **J-integral**: J-integral concept was first introduced by Rice. It is an energy based path independent integral equivalent to decrease in potential energy per every increment of crack extension. It is also representative of stresses and strains at the tip of notches and cracks in elastic or non-linear elastic materials. For elastic region, it is equivalent to strain energy release rate (G) and in non-linear region, it is a function of area under load-displacement curve.

J- integral approach is for non-linear elastic response and therefore reversible deformations. True plastic deformation processes are irreversible, thus energy dissipated is not transformed to strain or potential energy. An actual material response can be used as a special case for this approach assuming there is no unloading during the crack extension process. But during crack growth, the newly formed crack faces are completely unloaded from high yield stresses. Therefore, J principle is suitable upto beginning of crack extension and not for crack growth. In such cases, this non-linear elastic energy release rate can be

used for elastic-plastic energy release rate. J-integral can be viewed as energy parameter comparable to strain energy release rate (G) and stress intensity parameter comparable to stress intensity factor (K).

In a dynamic loading condition, polymer composites are assumed to behave linearly and thus above parameters can be related using basic principles of linear elastic fracture mechanics. In this project, J-integral and COD parameters are used to calculate fracture toughness(K) of composite material. Both the approaches are implemented as explained in the following sections

1. Crack opening displacement method

Dynamic stress intensity factor is calculated from static relations for stress intensity factor and crack opening displacement(COD) using the following Equ.(3.2)

$$K_i(t) = \frac{\pi}{\sqrt{2\pi r}} u(t) \frac{\omega_1 \omega_2}{\omega_1 + \omega_2} \frac{1}{a_{22}} \quad (3.2)$$

where

r is the distance from crack tip where COD is measured

$\phi_j = i\omega_j$ and ϕ is derived as follows,

Governing equation for an orthotropic plane stress composite material is:

$$\frac{\partial^4 \phi}{\partial x^4} + \frac{2b_{12} + 2b_{66}}{b_{22}} \frac{\partial^4 \phi}{\partial x^2 \partial y^2} + \frac{b_{11}}{b_{22}} \frac{\partial^4 \phi}{\partial y^4} = 0$$

where

ϕ represents four roots of fourth order equation given above

$$b_{11} = 1/E_1, \quad b_{12} = -\nu_{12}/E_1 = -\nu_{21}/E_2$$

$$b_{22} = 1/E_2, \quad b_{66} = 1/G_{12}$$

2. Strain energy release rate method

Strain energy release rate is the amount of energy dissipated during fracture propagation in creating new surfaces. Energy supplied at the crack-tip for it to grow is balanced by energy dissipation in form of energy release rate during fracture phenomena. J-integral as given in Equ.3.3 ?? is for a non-linear elastic or elastic-plastic material assuming no unloading conditions. It is independent of path around the crack and can be used to calculate K by assuming a path very near to notch tip. This is equivalent to strain energy release rate for an elastic material subject to quasi-static loading.

$$J = \int_{\Gamma} \left(W n_1 - T_i \frac{\partial U_i}{\partial x_1} \right) ds \quad (3.3)$$

However for dynamic cases, the path independent property of J-integral is no longer observed as the stress waves reaching one contour may not have reached to the next contour. Thus it becomes a time dependent and also path dependent function. Dynamic problems are unsolvable for elastic plastic growth as considerable unloading is expected to occur. It is still meaningful to derive expressions for path independent J-integral for non-linear elastic materials [22]. For a crack propagating in x-direction with a speed \dot{a} , dynamic J-integral can be expressed as given in Equ.3.4.

$$J = \int_{\Gamma} \left\{ \left(W + 1/2 \rho \dot{a}^2 \frac{\partial U_i}{\partial x_1} \frac{\partial U_i}{\partial x_1} \right) n_1 - T_i \frac{\partial U_i}{\partial x_1} \right\} ds + \int_{\Omega} \rho \left(\ddot{u}_i - \dot{a}^2 \frac{\partial^2 u_i}{\partial x_1^2} \right) \frac{\partial U_i}{\partial x_1} dA \quad (3.4)$$

where,

Γ = contour path surrounding the crack-tip from lower crack flank to upper flank

W = Strain energy density

ρ = mass density

u_i, \ddot{u}_i = displacement and acceleration

n_i = unit outward normal to contour Γ

T_i = traction on Γ

Ω = area bounded by Γ

Dynamic J-integral defined till the point of crack growth initiation for non-linear as well as elastic-plastic material is given using Equ.3.4 taking crack velocity, \dot{a} equal to zero which reduces the terms to give Equ.3.5 [23]. Therefore, dynamic J-integral is evaluated by adding an additional component equivalent to area (bounded by assumed contour (Γ)) integral of kinetic energy density to component having potential and strain energy density line contour (Γ) integral values.

$$J = \int_{\Gamma} \left(W n_1 - T_i \frac{\partial U_i}{\partial x_1} \right) ds + \int_{\Omega} \rho \ddot{u}_i \frac{\partial U_i}{\partial x_1} dA \quad (3.5)$$

Once critical J-integral value is calculated using FEM, this project will make use of Equ.(3.6),(3.7) and (3.8) for orthotropic material under quasi-static loading to obtain approximate results for fracture toughness values[24].

$$J = G \quad (3.6)$$

$$G_I = \frac{K_I^2}{\sqrt{2E_1E_2}} \left[\left(\frac{E_1}{E_2} \right)^{1/2} + \frac{E_1}{2G_{12}} - \nu_{12} \right]^{1/2} \quad (3.7)$$

$$G_{II} = \frac{K_{II}^2}{E_1\sqrt{2}} \left[\left(\frac{E_1}{E_2} \right)^{1/2} + \frac{E_1}{2G_{12}} - \nu_{12} \right]^{1/2} \quad (3.8)$$

D. Finite element analysis

Fracture toughness parameters required for this project- J and COD are obtained by using finite element codes in ABAQUS. Non-linear finite element module is used to study impact event on three point bend sample. Crack in SENB 2d model is represented using contour integral spanning full specimen of width(20mm). Concentrated point loads in the form of loading history(P vs t as obtained from SHPB) is given as loading condition at node representing the loading point.

Table I. Material elastic constants

Material	Density (kg/m ³)	E ₁ (GPa)	E ₂ (GPa)	ν_{12}	G ₁₂ (GPa)	G ₁₃ (GPa)	G ₂₃ (GPa)
Carbon epoxy laminate	1505	107.70	8.10	0.34	3.85	3.85	3.02
Fiberglass epoxy laminate	1720	28.50	8.17	0.31	2.52	2.52	3.13
Mat reinforced fiberglass epoxy laminate	1610	21.60	8.04	0.32	2.59	2.26	2.67

Properties of three polymer composites are provided by suppliers as given in Table I. Fibers are noted as parallel to direction 1. Dynamic implicit solver is employed to analyze the impact event in micro seconds. Singular elements are used at the crack for contour integral module to obtain J-integral output which is path independent thus number of nodes is determined according to the number of contours desired around the crack tip. First contour lies at the crack tip and is preferably ignored. Output can be requested in the form of energy release rates(J) or stress intensity factors(K) or both at each of the contours.

1. COD and ERR calculation based on LEFM

Linear elastic fracture mechanics assumes a material to behave in almost perfectly elastic manner. Therefore, assuming that there will be no yielding or very small yielding near the crack tip, stresses near tip will become infinite on application of load. Using this assumption, fracture mechanics study becomes trivial and equations for toughness parameters like energy release rate, J-integral, COD can be derived easily depending on boundary conditions. In this project, high velocity impact event is assumed to make the composite material behave in a brittle manner and LEFM theory can be applied.

COD is a useful fracture parameter and can be divided into elastic and plastic component. Elastic component is directly related to stress intensity factor and can be computed using LEFM theories. The other plastic component is neglected for this problem as it is assumed material is in linear elastic range till the moment of crack propagation initiation. Therefore, 2d orthotropic elastic properties for a laminate in plane stress conditions is given as material model for finite element simulations. COD is monitored at a node which is approximately at the same distance as the strain gauge near the notch tip in the experiments. Strain gauge being approximately at 1mm from notch end, $COD(u(t))$ is measured at a distance of $r=1\text{mm}$, used in Equ.(3.2) to obtain the stress intensity factor values at each time step. It is not required to use contour integral functionality for COD output.

J-integral is another important and useful parameter which is again not limited by bounds of LEFM theory. It can be subdivided into elastic and plastic components but due to assumption of elastic response of material, plastic part can be ignored. Also, it can be related to energy release rate as per the boundary conditions and specimen geometry. So, in this project, J-integral output of finite element simulation

is assumed equivalent to strain energy release rate. Strain energy release can be related to stress intensity factor by Equ.(3.7)and (3.8) depending on the modes of fracture and boundary conditions.

2. COD and ERR calculation based on damage model

Composites materials are considered to be non-linear in nature. The non-linearity tends to decrease as strain rates are increased and assuming it to be completely elastic may prove to be an over assumption of material properties. Therefore, using Hashin damage model for fiber reinforced model may provide better values of dynamic fracture initiation toughness. This study of non-linear material response will take care of all degradation processes occurring in the composite material before it gives away and crack starts to propagate. Damage can occur in many ways and all this can be incorporated in a damage model by using a user defined material subroutine (UMAT) or by using available Hashin damage model as explained in Appendix.A.

Three dimensional composite section(assuming unit thickness) is used with 40 plies stacked at required 90° angles and a dynamic finite element solver is implemented to model the impact. Average crack opening displacement is recorded at node 1mm from the crack tip and stress intensity factor is calculated as a function of time using Equ.(3.2).

Strain energy release rate(G) is energy required to propagate a crack therefore it can be assumed that energy consumed in damaging composite material until the crack starts to propagate is equivalent to strain energy release rate required to initiate cracking. It is based on an important assumption that all the damage is concentrated near the crack tip until the crack starts to propagate, at a threshold value of stress intensity, as also indicated by Mandell [17]. This damage dissipation energy function is incorporated in ABAQUS solver as explained in Appendix.A. Strain energy release

rate obtained is used to compute stress intensity factor as a function of time as given in Equ.(3.7),(3.8), depending on the boundary conditions.

Therefore, this project not only provides a methodology to determine the dynamic fracture initiation toughness of different unidirectional laminates. It also compares various approaches that can be used to calculate values of fracture toughness parameters. Finally, microscopic observation near the crack-tip provides further insights into the dynamic damage event.

CHAPTER IV

EXPERIMENTAL RESULTS

A. Quasi-static test results

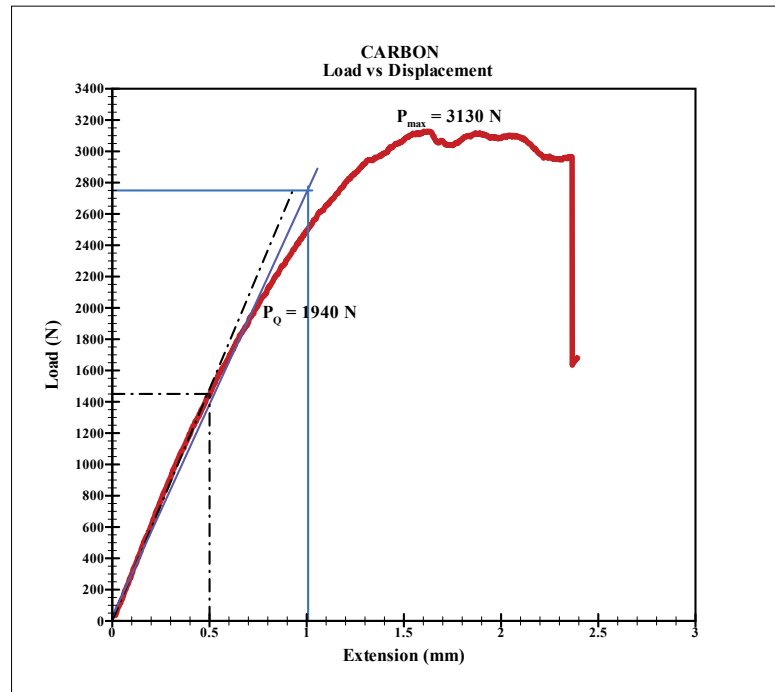
Quasi-static tests are performed as a reference to gain knowledge on composite material response with a change in loading rates. A constant rate of loading is maintained and sample data is recorded till it reaches the failure point. Three point bending configuration (Fig. 6) for flexure loading is used for both Mode-I and Mode-II testing. Observations made for different fracture modes are given in following subsections.

1. Mode-I quasi-static test

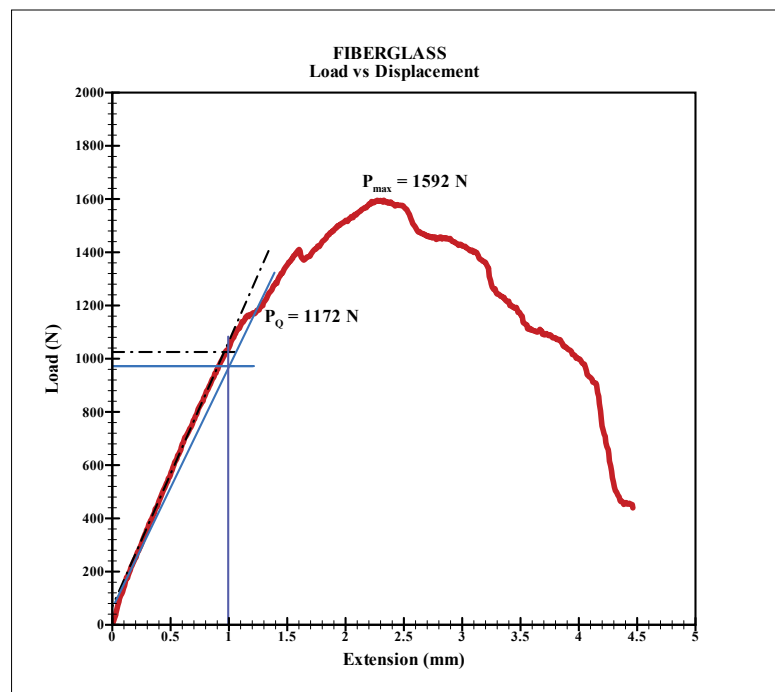
Quasi-static tests of composite laminates show linear behavior at first and then it starts deviating to show non-linear characteristics. Using standard procedures as explained in ASTM E399 for measuring quasi-static fracture toughness, 95% value of slope of the linear portion is taken and its intercept on load axis gives peak load P_Q to be used in Equ.(3.1). Fig. 11 shows data for carbon-epoxy and fiberglass-epoxy SENB specimen, with fibers aligned perpendicular to notch, tested for Mode-I quasi-static fracture toughness. It is worth noting that P_Q values of carbon-epoxy sample is 62 % of maximum load value while for fiberglass-epoxy this value is 75 %. Fiberglass-epoxy samples record a more non-linear behavior than carbon-epoxy samples.

2. Mode-II quasi-static test

Same procedure is followed for Mode-II testing to find P_Q as for Mode-I. Local deformation at the point of loading is observed at location of load application followed



(a) Carbon Mode-I quasi-static test data



(b) Fiberglass Mode-I quasi-static test data

Fig. 11. Load vs displacement plot of SENB sample under quasi-static loading

Table II. Maximum load endured P_{max} and Peak loads P_Q at fracture initiation for different composite laminates and modes of fracture

Material	Mode of fracture	Rate of loading (mm/min)	P_{max} (N)	P_Q (N)
Carbon epoxy	Mode-I	0.1	3130	1940
	Mode-II	0.1	6400	4490
Fiberglass epoxy	Mode-I	0.1	1592	1172
	Mode-II	0.1	5220	3400

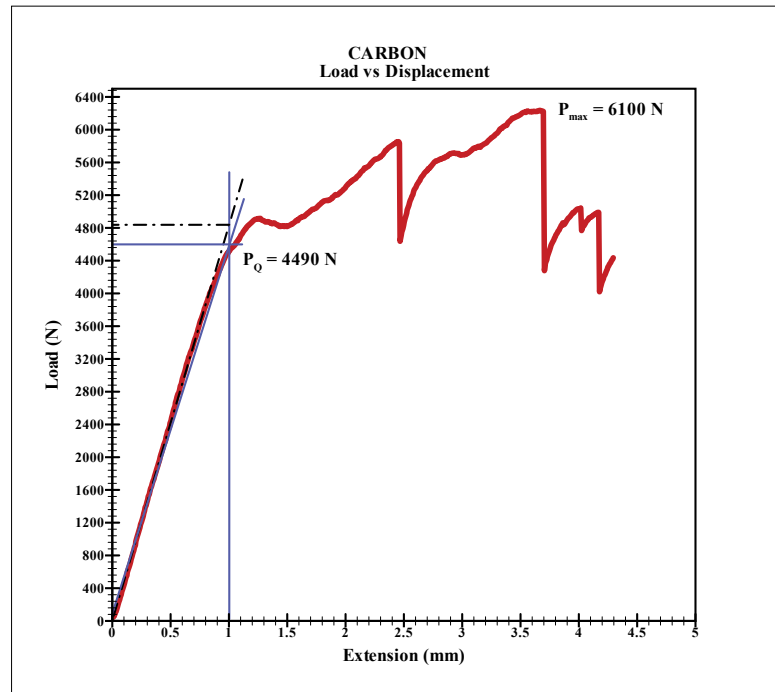
by bending of specimen. Load vs displacement for carbon-epoxy ENF sample, with fibers running parallel to pre-existing crack, is shown in Fig. 12. Again carbon-epoxy shows more linear characteristics as compared to fiberglass-epoxy response. Values of P_Q for various samples tested are listed in given in Table II.

B. Impact tests

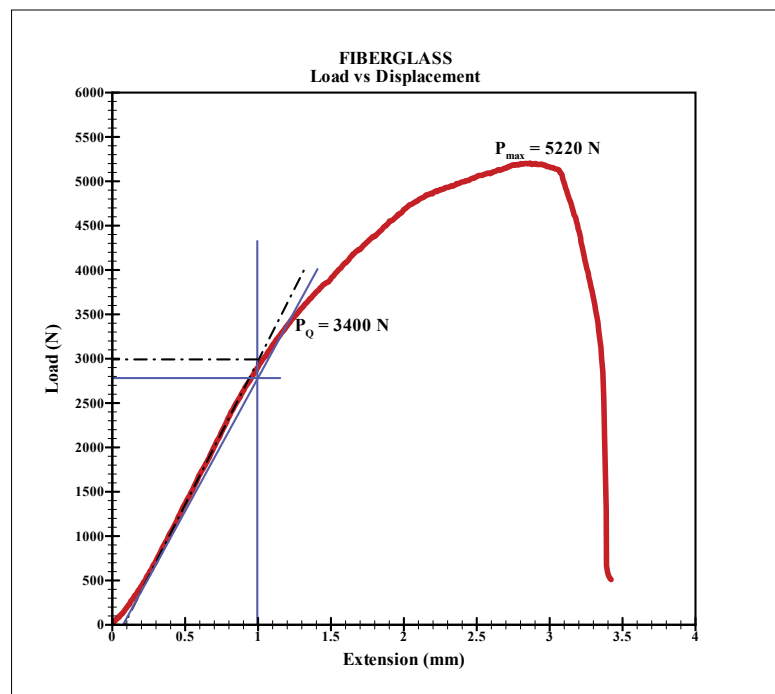
Impact tests on SHPB apparatus are performed at CIDESI to give following fracture toughness parameters. SHPB set-up gives:

- Strain gauge voltage signals recorded during the impact
- Velocity at impact
- Initiation of crack propagation instant

Incident and reflected pulses recorded by oscilloscope are shifted to a common reference point that is to the instant at which impacting compressive wave reaches the specimen surface. It takes around $187\mu s$ for an incident wave to reach sample surface from the point where strain gauge is attached and it takes $375\mu s$ to record the



(a) Carbon Mode-II quasi-static test data



(b) Fiberglass Mode-II quasi-static test data

Fig. 12. Load vs displacement plot of ENF sample under quasi-static loading

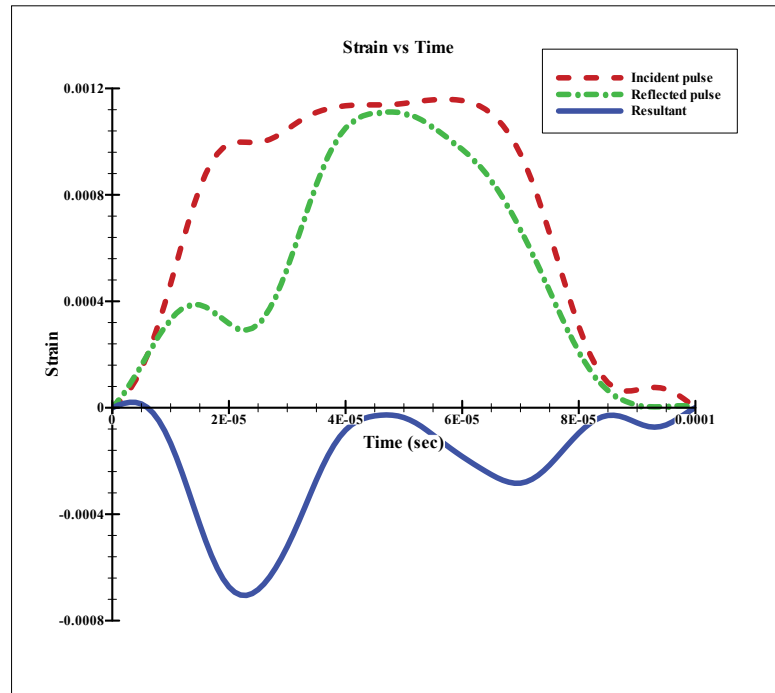


Fig. 13. Strain pulses as obtained in impact testing

reflected wave at the strain gauge on incident bar. Using Equ.(2.2), resultant compressive wave on specimen obtained is as shown in Fig. 13. The resultant signal is converted to loading history with the help of MATLAB code (courtesy CIDESI) given in Appendix.B. Same steps are repeated for Mode-I as well Mode-II testing as described in following sub-sections.

Typical crack gauge signal recorded by oscilloscope is seen in purple colored channel three output in Fig. 10. This pulse is used to detect crack initiation time in fracture event. Positioning of strain gauge is in such a way that the first peak is observed to be in compression for SENB type geometry. The time instant of this very first peak is noted as the time of initiation of crack. This time instant includes time for wave to travel in incident bar ($187\mu\text{s}$) and in uncracked length of sample to reach the crack tip. Wave travel time can be calculated by obtaining the wave

speed c_d in material and distance of travel. Parameter c_d can be easily calculated using material elastic constants as given in Equ.(4.1) [25]. Fiber orientation should be taken into account by transforming the stiffness matrix such that direction-1 is parallel to wave propagation direction. c_d obtained for different materials and fiber orientation is presented in Table III.

$$c_d = \sqrt{c_{11}}c_s \quad (4.1)$$

where

c_d is dilatational wave speed

c_s is velocity of in-plane shear wave

For a plane stress condition

$$\begin{aligned} c_{11} &= \frac{E_{11}}{G_{12}[1 - (E_2/E_1)\nu_{12}]^2} \\ c_s &= \sqrt{G_{12}/\rho} \end{aligned}$$

G_{12} is in-plane shear modulus

and, ρ is mass density

Table III also presents the time for a wave to travel a distance of 10mm in a given material. Therefore using this wave travel time for carbon-epoxy sample and Fig. 14, time of crack initiation is observed around $27\mu s$. Similarly, varying wave speeds and travel times are obtained for different test cases as given in Table III.

In Dr.Rubio's previous work [26], dynamic fracture toughness of the same carbon-epoxy laminate material is found in velocity range of 15-16 m/s. In this project,

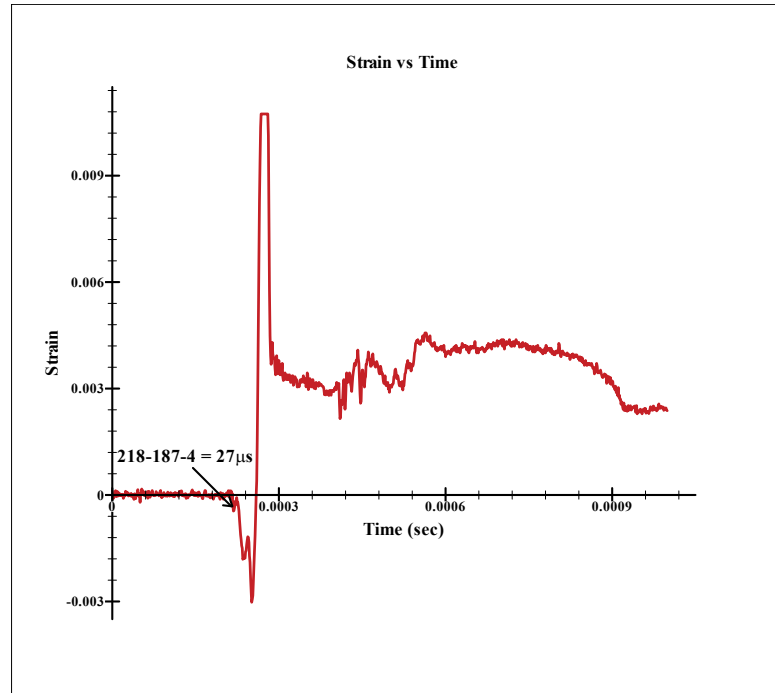


Fig. 14. Crack tip strain gauge pulse showing time of initiation of crack

Table III. Wave speeds and traveling times making a particular angle to laminate fiber direction

Material	Angle of wave wrt fiber direction ($^{\circ}$)	c_d (m/sec)	Time taken to travel 10mm distance (μ s)
Carbon epoxy	90	2329.00	3130
	60	2497.66	6400
Fiberglass epoxy	90	2210.90	1592
	60	2155.80	5220
Mat reinforced fiberglass epoxy	90	2279.20	1592
	60	2313.30	5220

similar sample dimensions are tested for Mode-I but at a lower velocity range of 9 m/s to 14 m/s. This range of data will help in estimating a trend in material response with change in velocity at impact. In addition, specimens are tested for Mode-II fracture toughness.

1. Mode-I impact test

Impact testing for Mode-I fracture toughness are conducted using SENB geometry. There is a pre cut notch perpendicular to fiber orientation. SENB specimen is impacted at midspan of uncut side to extend the notch due to flexure loads on opposite end.

Loading history obtained from Mode-I impact fracture initiation test of each material type is shown in Fig. 15. The fracture initiation time is calculated as given in Fig. 14 and using wave velocity evaluated for propagation perpendicular (90°) to fiber direction.

Examining the broken pieces it can be observed that crack initiates along the fiber length till stresses become high enough to cause fiber failure as shown in Fig. 16. The crack propagates across fibers breaking the specimen into two. However, this is only observed in carbon samples made from prepregs. Fiberglass samples absorb all the impact energy and as can be seen in Fig. 17. Local material degradation near crack-tip does occur but the crack is restricted to propagate and break the sample into two.

2. Mode-II impact test

The procedure to obtain load-time plot in this testing configuration is similar to the method defined for Mode-I impact testing problem. But, ENF impact tests reveal lack of symmetry in the two transmitter signals as shown in Fig. 18. This is due

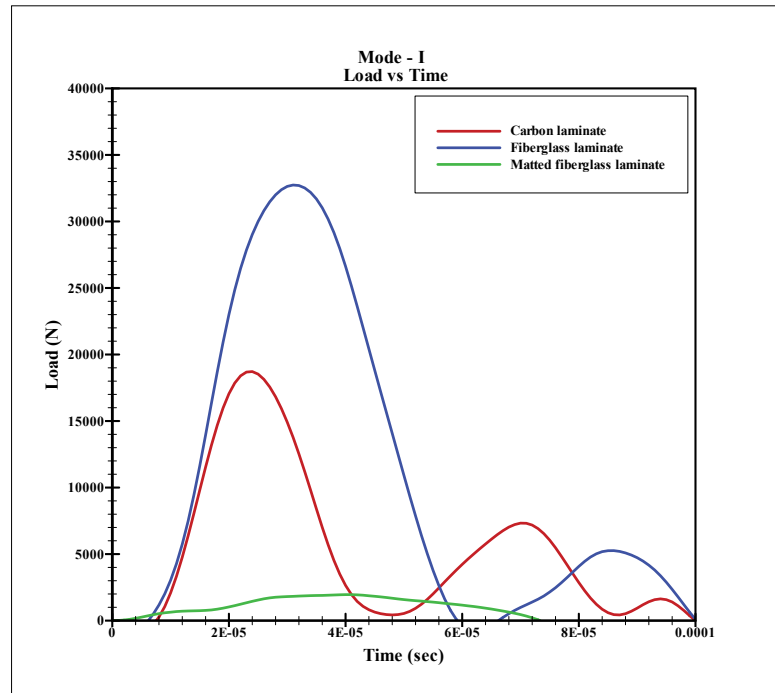
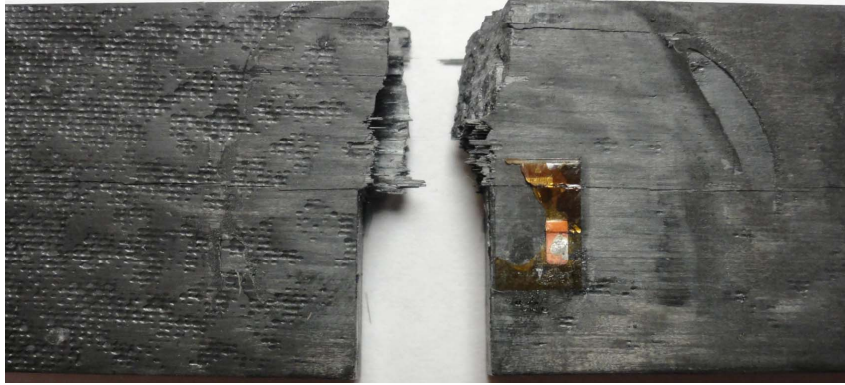


Fig. 15. Load vs time plot of various PMCs for Mode-I impact tests

to the presence of an end notch which makes the sample geometry conditions non-symmetric unlike in Mode-I SENB samples. The loading history obtained for ENF type of geometry of different materials with fibers aligned parallel to notch of 30mm is shown in Fig. 19.

The shortest path for stress wave to reach crack tip in ENF specimen will be at 60° to direction of fiber orientation. So the wave travel time is calculated for a distance of approximately 20mm and at an angle of 60° to the reference axis in fiber direction. For a carbon sample, time taken to reach crack tip is calculated to be $8\mu\text{s}$. The crack initiation time is recorded, for use in simulation, following same steps as indicated in Fig. 14.

It is interesting to observe in both Mode-I and Mode-II testing, crack tip strain gauge signal was registered before the transmitter signal triggered. Therefore, crack



(a) Top view showing fiber bridging



(b) View of cracked faces

Fig. 16. Pictures of impact damaged carbon-epoxy laminate specimen



Fig. 17. Impact damaged fiberglass-epoxy laminate



Fig. 18. Strain gauge signals recorded for Mode-II impact tests

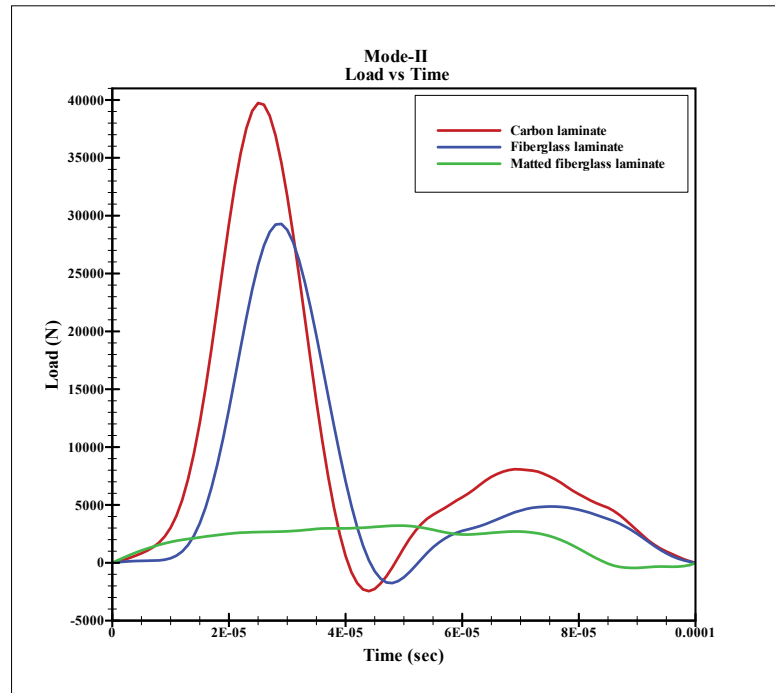


Fig. 19. Load vs time plot of various PMCs for Mode-II impact tests

begins to initiate before the wave is transmitted to transmitter bar as can be seen in Fig. 10 and Fig. 18. Therefore, transmitted pulse is not used in equations to compute loading curve (P vs t). Only $P_i(t)$ is used in the simulations as $P_t(t)$ has no effect.

Final steps to calculate the fracture toughness values using above experimental data are outlined in the following chapter.

CHAPTER V

FRACTURE TOUGHNESS CALCULATIONS

The objective of this project is to develop a numerical-experimental approach for finding dynamic fracture toughness of polymer composites. Parameters obtained from experiments are used in finite element analysis and formulae to finally give an estimate of fracture initiation toughness property. Various methods used are explained in subsequent sections.

A. Quasi-static fracture toughness

Value of peak load (P_Q) at the time of crack initiation depends on material properties as can be seen in Fig. 11 and Fig. 12. Therefore, it is an important parameter that can be used directly to calculate fracture related properties of samples. There are also finite element codes to calculate fracture toughness values as outputs. So, parameter P_Q has been used in following two ways to obtain fracture toughness.

From relation: P_Q is directly used in Equ.3.1 to calculate quasi-static fracture toughness values(K_Q). Following are the values of variables to be used in relation Equ.3.1,

P_Q (Table II), load at crack initiation and is calculated as shown in Fig. 11

S , span length is the supported length of the samples between the two supporting end of three point bend fixture, = 80mm

a , length of pre-crack in the sample, = 10mm

W , total width of sample where notch is cut, = 20mm

B , thickness of sample = 6.44mm for carbon, = 6.90mm for fiberglass

Finite element analysis: ABAQUS standard solver is implemented with three-point bend model having a 0.10 mm/min loading rate boundary condition . Energy

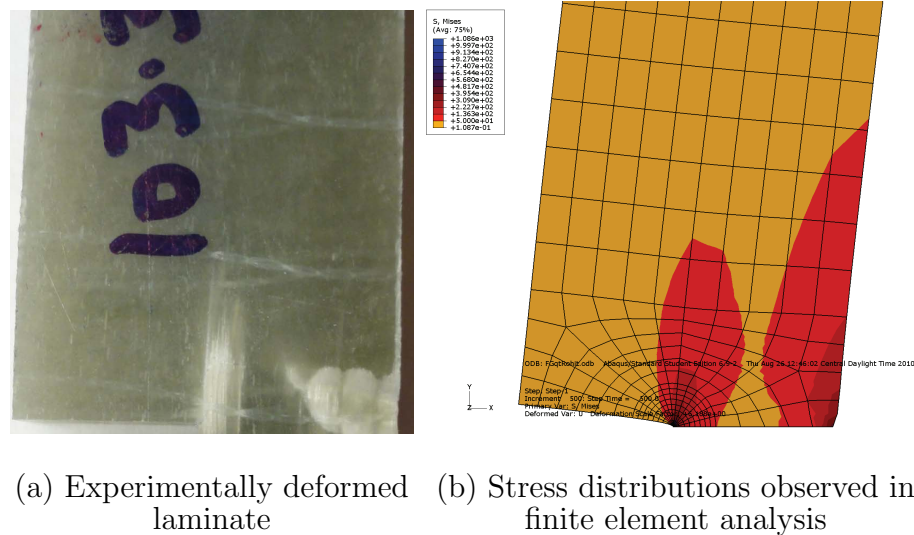
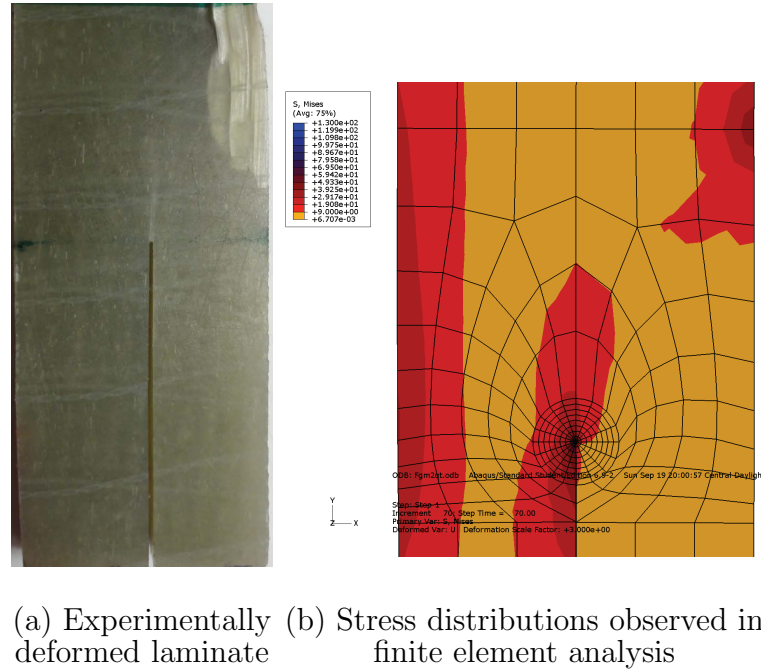


Fig. 20. Comparison of stress distributions observed in fiberglass-epoxy laminate tested for Mode-I quasi-static fracture toughness

release rate output is requested in the pre-cracked region using contour integral functionality. From experimental data, time instant corresponding to occurrence of load P_Q is noted and energy release rate corresponding to that particular time instant is reported as critical strain energy release rate (G_C). Equ.3.7 and 3.8 is used to obtain K_C depending on fracture mode being tested. Von Mises stress distributions from finite element analysis tally with deformations observed at the end of quasi-static tests as shown for fiberglass laminates in Fig. 20 and Fig. 21 for Mode-I and Mode-II respectively. Thus, finite element code used is a good approximation of the real experimental phenomena.

1. Mode-I fracture toughness

ABAQUS standard code is used with orthotropic plane stress material properties (Table I) and SENB model with dimensions as shown in Fig. 6. Quasi-static tests in three point bend fixture are modeled with two supports and a loading boundary condition. Crack is described as previously and contour integral outputs are requested



(a) Experimentally deformed laminate (b) Stress distributions observed in finite element analysis

Fig. 21. Comparison of stress distributions observed in fiberglass-epoxy laminate tested for Mode-II quasi-static fracture toughness

Table IV. Mode-I quasi-static fracture toughness values (K_{IC})

Material	K_{IC}	G_{IC}	K_{IC}
	From ASTM standard ($\text{MPa}\sqrt{m}$)	From FEM (mJ/mm^2)	From G-K relation ($\text{MPa}\sqrt{m}$)
Carbon	25.00	24	29.00
Fiberglass	10.80	4	7.75

Table V. Mode-II quasi-static fracture toughness values (K_{IIC})

Material	G_{IIC}	K_{IIC}
	From FEM (mJ/mm ²)	From G-K relation (MPa√m)
Carbon	0.20	1.41
Fiberglass	0.18	1.20

for five contours in this case. Output in the form of energy release rates is independent of contour path. The time instant recorded for P_Q is used to find the critical strain energy release rates ($J=G$). The values of G_{IIC} and K_{IIC} so obtained by using a standard equation and numerical simulations output are given in Table IV for SENB type geometry .

2. Mode-II fracture toughness

Fracture toughness values obtained using equation and simulation is within range of 10%-30% as seen for Mode-I results above. Therefore, simulations can be relied upon to estimate Mode-II fracture toughness property. ABAQUS standard solver is employed as above but ENF geometry lacks symmetry and hence complete geometry with two supports is modeled. P_Q (Fig. 12) obtained earlier is used to find time instant of crack initiation and critical strain energy release rate (G_{IIC}) is recorded at that instant. K_{IIC} calculated for both carbon and fiberglass are listed in Table V.

B. Dynamic fracture initiation toughness

ABAQUS non-linear implicit code is used to simulate three-point bend SHPB impact tests. Loading boundary condition are obtained from loading history from experi-

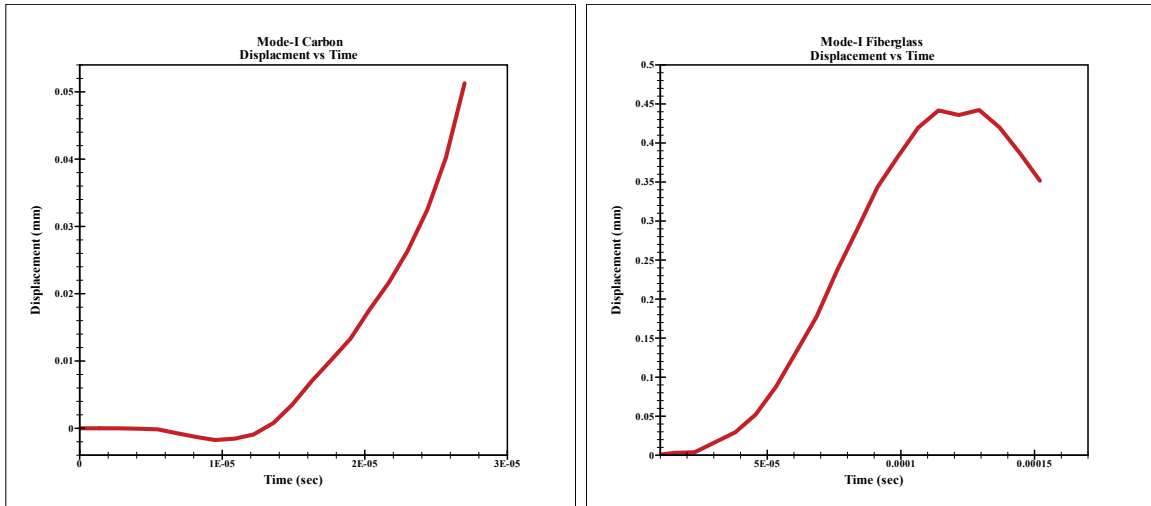
ments as given in Fig. 15 and 19 and stress intensity factor is calculated using crack opening displacement or energy release rate outputs. Stress intensity factor value at the time of initiation of crack as recorded by strain gauge, at crack tip, is the fracture toughness property of samples being tested.

1. Mode-I dynamic fracture toughness

Finite element analysis, using orthotropic plane stress material properties, is conducted for full SENB geometry to obtain parameters like crack opening displacement ($u(t)$) and strain energy release rate (J) for use in relations for calculating dynamic fracture initiation toughness. The two methods employed are explained as follows.

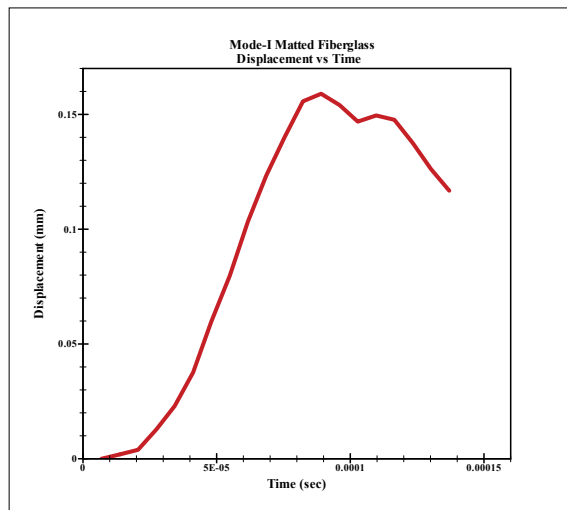
Crack opening displacement Crack opening displacement(COD) is measured at a node 1mm from crack tip which is approximately the strain gauge position in impact tests. This displacement perpendicular to crack axis is recorded as a function of time as shown in Fig. 22. Similarly, only carbon-epoxy laminates are evaluated using damage model to understand the effect of non-linear response of a damage model. The difference in stress intensity factor values obtained for the same carbon-epoxy laminate from two different models is shown in Fig. 23. Displacement, $u(t)$ is then used in Equ.3.2 to evaluate the stress intensity factor variation with time taking $r=1\text{mm}$. Calculated stress intensity factor(K) vs time output is shown in Fig. 24. Value of K at instant of crack initiation is recorded as dynamic fracture initiation toughness (K_{ID}) of the material.

Finite element analysis As described for quasi-static toughness calculations, five contour integrals are defined around the crack tip in ABAQUS simulations. For dynamic loading as shown in Fig. 15, path dependent energy release rate output(J) is found using LEFM theory for crack analysis. Adding a factor for kinetic energy density gives value of path independent dynamic J-integral as given in Equ.3.5. Ki-



(a) Carbon laminate

(b) Fiberglass laminate



(c) Mat reinforced fiberglass laminate

Fig. 22. Crack opening displacement history from impact simulation of SENB samples

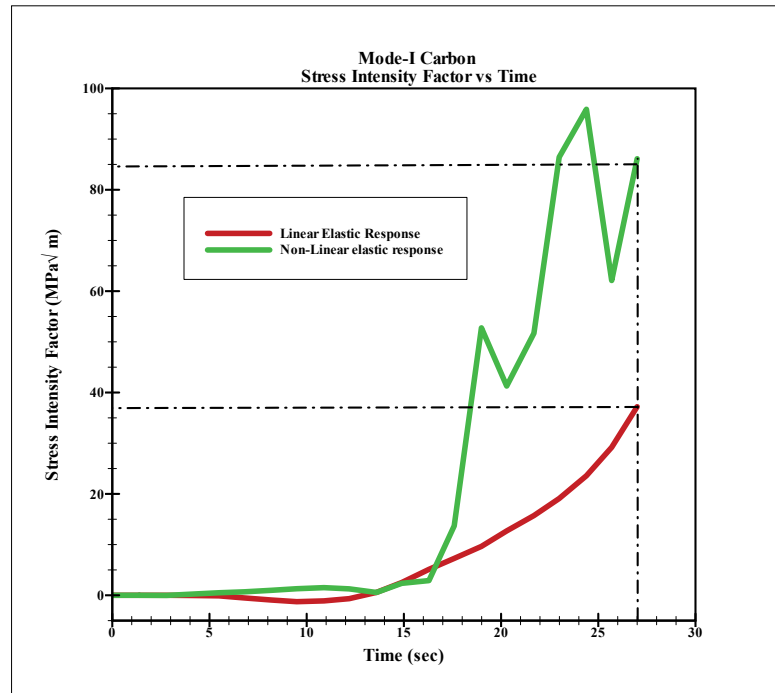
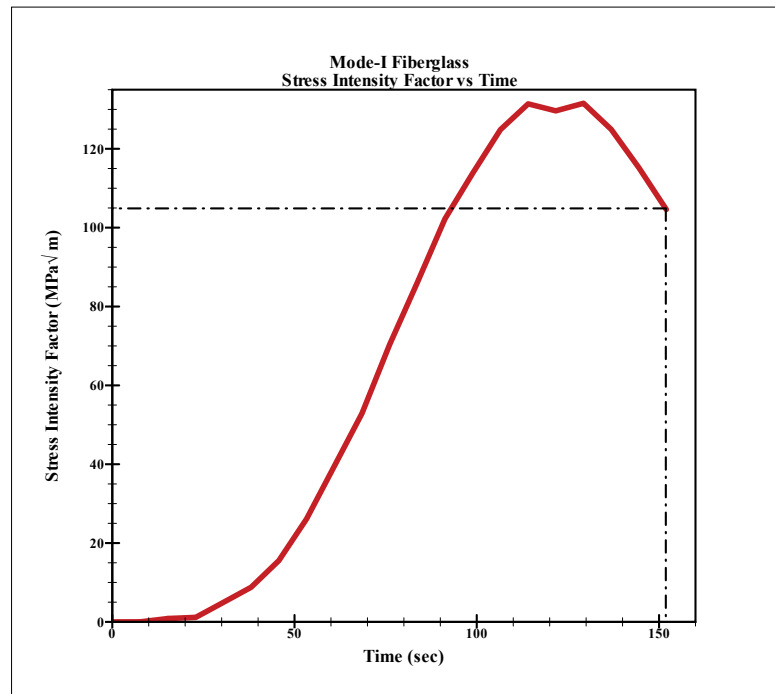


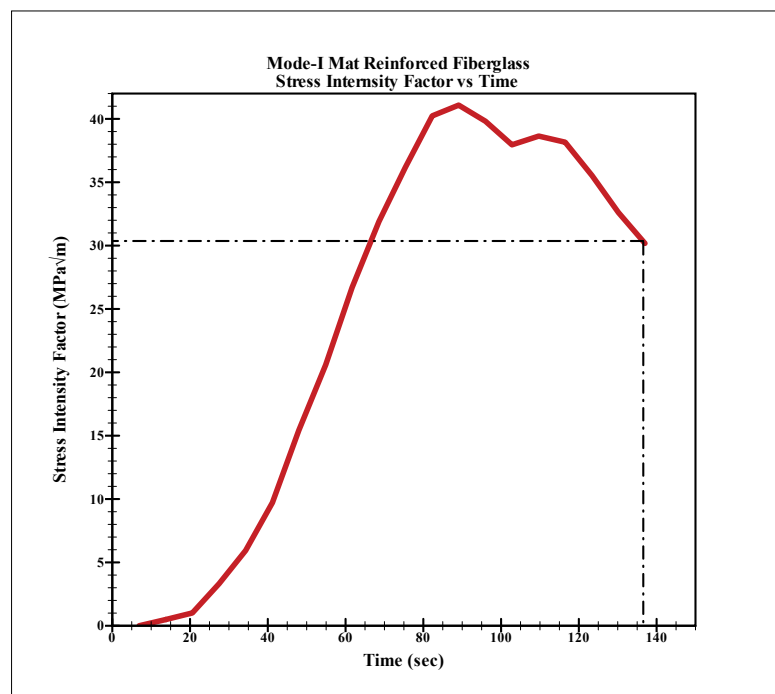
Fig. 23. Mode-I stress intensity factor vs time for carbon comparing material models

netic energy density is measured in area of radius 0.20mm near crack tip enclosed by second J-integral contour. Similarly, using a damage model, damage dissipation energy output is measured for an area of 0.20mm around the crack tip. This localized damage dissipation energy density is considered equivalent to critical strain energy release rate(G_C) at the instant of crack propagation.

Critical energy release rate is J-integral value calculated at instant of crack propagation. Assuming linear elastic material response, statics equation Equ.3.7 is used to determine Mode-I dynamic fracture toughness (K_{ID}) property of the material tested. Energy release rate variation with time for all the material types are shown in figures below Fig. 25. Only carbon-epoxy is tested with non linear damage model and to compare, the values are as shown in Fig. 26. Using the plots and equations as explained above, results for Mode-I fracture initiation toughness of various laminates are summarized in Table VI.

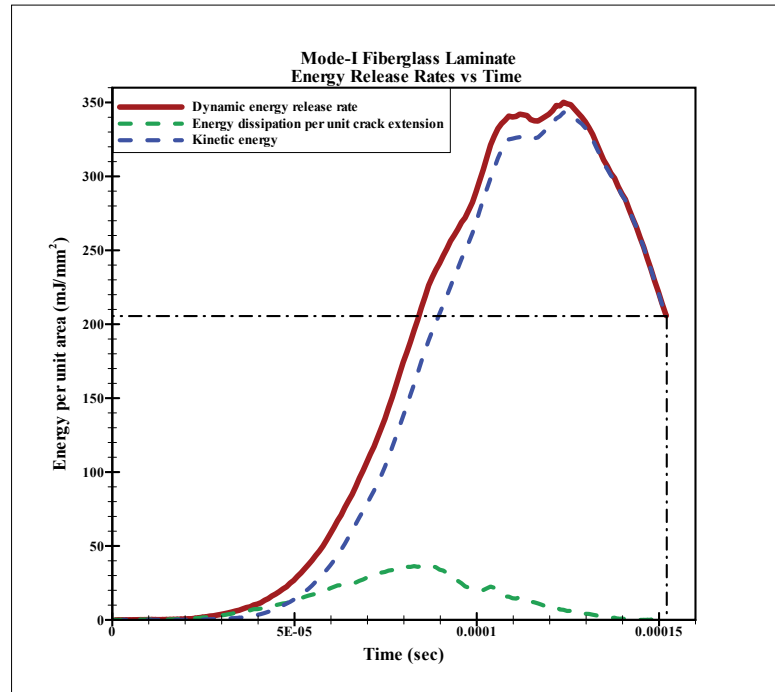


(a) Fiberglass laminate

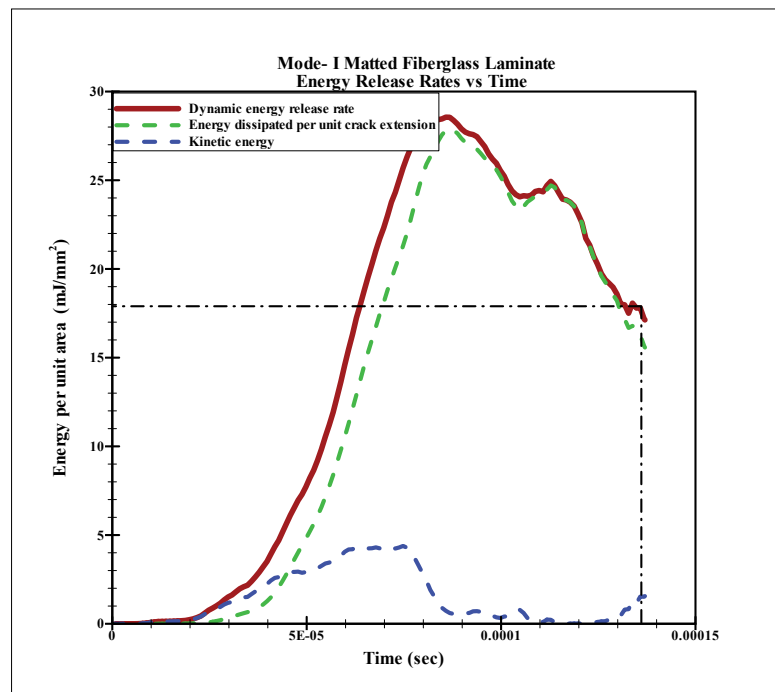


(b) Mat reinforced fiberglass laminate

Fig. 24. Mode-I stress intensity factor history of fiberglass and matted fiberglass assuming linear elastic material model



(a) Fiberglass laminate



(b) Matted fiberglass laminate

Fig. 25. Mode-I energy release rate vs time for fiberglass and matted fiberglass laminates using linear elastic model

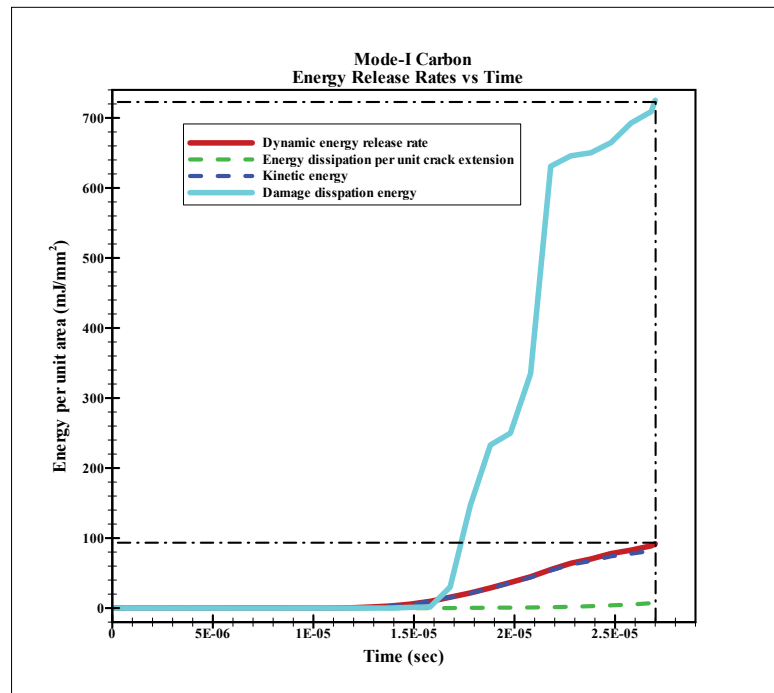


Fig. 26. Mode-I energy release rate vs time for carbon using different material models

Table VI. Mode-I dynamic fracture toughness values (K_{ID})

Material	Material model	Sample number	Velocity of projectile at impact (m/sec)	K_{ID} From COD (MPa \sqrt{m})	K_{ID} From FEM (MPa \sqrt{m})
Carbon laminate	Linear elastic	Sample-I	12.50	37.00	58.00
	Linear elastic	Sample-II	13.20	45.00	66
	Non-linear elastic	Sample-I	12.50	86.12	164.40
	Non-linear elastic	Sample-II	13.20	90.00	153.08
Fiberglass laminate	Linear elastic	Sample-I	13.24	104.60	51.80
	Linear elastic	Sample-II	10.42	335.00	138.00
Matted fiberglass laminate	Linear elastic	Sample-I	10.39	30.00	15.00

2. Mode-II dynamic fracture toughness

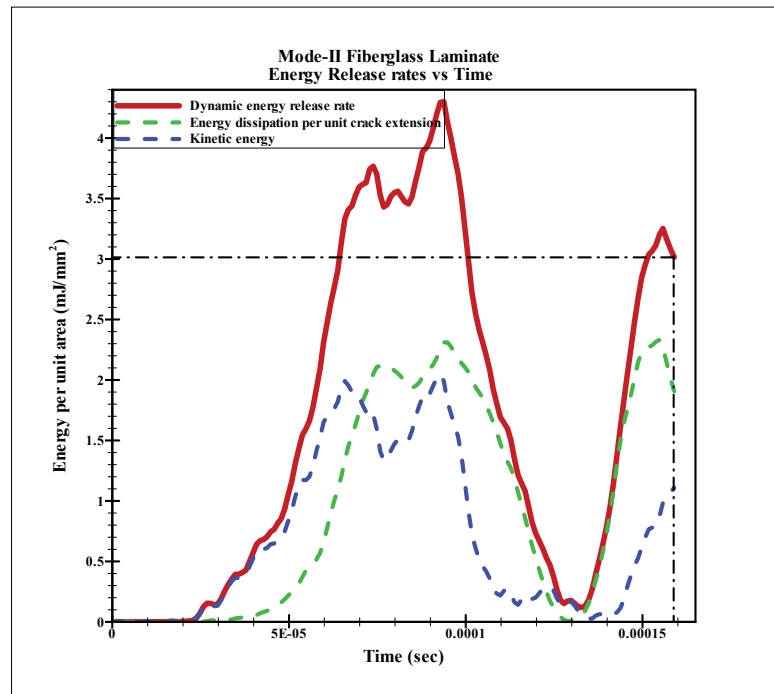
This project takes a step forward in finding Mode-II intralaminar fracture initiation toughness for polymer composites. As done in many previous studies, Mode-II is commonly calculated by finding the energy dissipated for crack extension. Therefore, using the same energy release rate methodology as explained above for Mode-I fracture toughness, Mode-II fracture toughness is determined. This method is again tested and compared for carbon-epoxy laminates to find the non-linear and more realistic composite response to impact force.

Simulation outputs in the form of dynamic J-integral for a linear elastic material model of fiberglass and matted fiberglass laminates are shown in Fig. 27. Carbon is also studied using a non-linear elastic damage model and is compared with linear elastic model in Fig. 28.

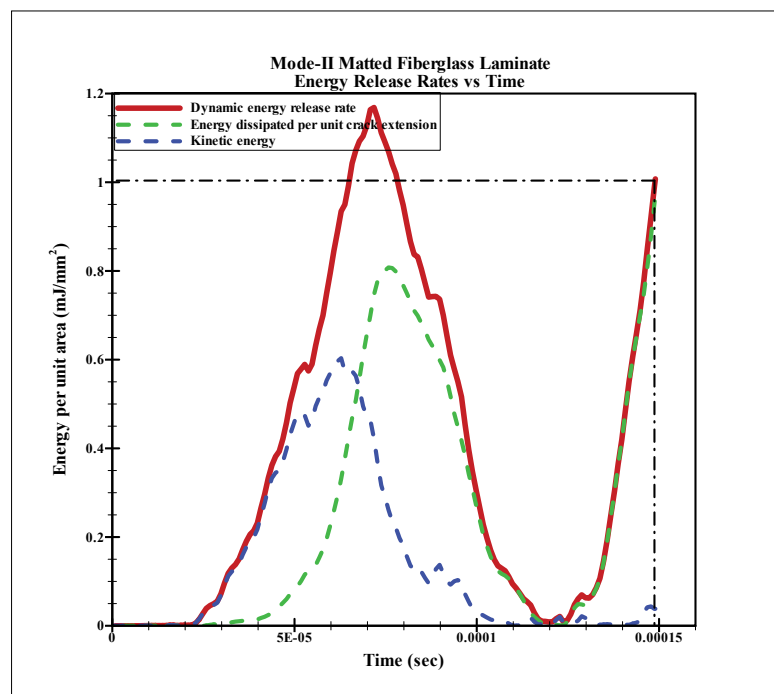
Finally, all the results obtained from simulated outputs are used to calculate Mode-II dynamic fracture initiation toughness (K_{IID}) as given in Table VII.

Table VII. Mode-II dynamic fracture toughness values (K_{IID})

Material	Material model	Sample number	Velocity of projectile at impact (m/sec)	K_{IID} From FEM ($\text{MPa}\sqrt{m}$)
Carbon Laminate	Linear elastic	Sample-I	11.91	43.01
	Non-linear elastic	Sample-I	11.91	90.18
Fiberglass Laminate	Linear elastic	Sample-I	10.42	4.19
	Linear elastic	Sample-II	10.42	7.57
Matted fiberglass laminate	Linear elastic	Sample-I	11.36	3.56
	Linear elastic	Sample-II	10.40	2.82



(a) Fiberglass laminate



(b) Matted fiberglass laminate

Fig. 27. Mode-II energy release rate vs time for fiberglass and matted fiberglass laminates using linear elastic model

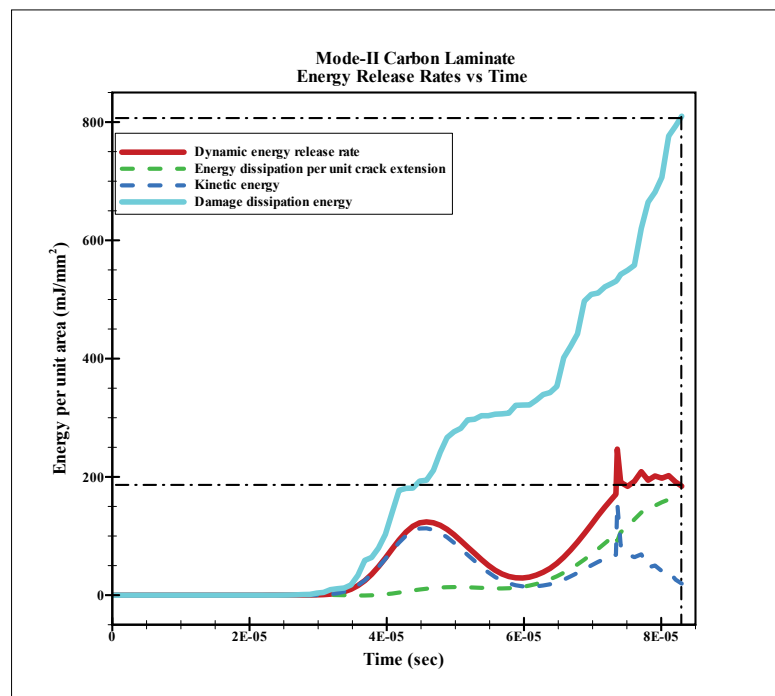


Fig. 28. Mode-II energy release rate vs time for carbon using different material model

CHAPTER VI

RESULTS AND DISCUSSIONS

This section discusses final results, reasons, various assumptions and their effect on final values obtained. Dynamic fracture toughness needs to be evaluated using a series of steps. Quasi-static fracture toughness testing of polymer composite materials is an effective means to confirm the trend in strain rate dependent material properties giving higher fracture toughness values for higher loading rate conditions. The numerical-experimental methods to achieve objective of this project are a means to enhance cost effectiveness over other approaches. Results calculated are based on many assumptions and thus will have deviations from expected values that can be explained by understanding material behavior, constituent material properties and their interactions with each other.

A. Discussion on quasi-static fracture toughness results

The method used to obtain quasi-static fracture toughness values is well documented and standardized in ASTM E399. The results show fracture toughness values of around $29 \text{ MPa}\sqrt{m}$ and $7.75 \text{ MPa}\sqrt{m}$ for carbon-epoxy and fiberglass epoxy laminates respectively. These numbers are consistent with the results obtained in previous studies [26]. Finite element standard analysis results using J-integral outputs show promising results very close to the results obtained from ASTM standard. Finite element code has been implemented using same assumptions of material properties and test conditions as for the standard relation. Thus both values were expected to be similar.

Inferring from similarity of values obtained using J-integral and ASTM standard methods for Mode-I testing, Mode-II fracture toughness values are evaluated using

only FEM analysis. Carbon-epoxy exhibit Mode-II fracture toughness value of around $1.41 \text{ MPa}\sqrt{m}$ and fiberglass-epoxy with a slightly lower number of $1.20 \text{ MPa}\sqrt{m}$. Explanation comparing various values obtained in this exercise are as follows:

1. Longitudinal load bearing fiber strength

Carbon fibers being tougher have the capability to bridge the crack opening response due to loading. Loading rates of $0.10\text{mm}/\text{min}$ ensures sufficient time for uniform load transfer to give superior properties of bulk mass. Matrix transfers the load to fibers and fibers can effectively sustain the loads upto their failure limits. This process can be approximated to a steady state loading condition and hence makes full use of fiber strength characteristics. Glass fibers have the capability to deform or yield more than carbon fibers before failure as can be seen in Fig. 11. But, fiber bridging being major load bearing factor is more efficient in carbon-epoxy laminates giving high fracture toughness values.

2. Thickness factor

Although plane stress conditions are assumed for calculated and simulated outputs, the experiments have been conducted on different sample thicknesses. As discussed in earlier chapters, fracture toughness is a thickness dependent parameter, giving highest values for plane stress conditions and lowest for plane strain. Region for this test condition can be put somewhere at an intermediate point on curve given in Fig. 2. Carbon-epoxy laminate being tested was measured to be 6.40mm whereas fiberglass laminate was around 6.99mm . This can be one contributing factor for lower fracture toughness results for fiberglass epoxy laminate sample when compared with a value of around $14 \text{ MPa}\sqrt{m}$ for 4.80mm thick prepreg fiberglass epoxy sample tested by Rubio et al.[26].

3. Manufacturing process

Another major factor influencing composite properties and its response is the manufacturing process. Tests were conducted on carbon-epoxy and fiberglass-epoxy samples prepared by different methods. Carbon-epoxy samples were made using prepreg curing whereas fiberglass laminates were prepared using hand lay-up process making it more prone to flaws like voids and inconsistent fiber matrix ratios. These are potential sites of stress accumulation and thus lower load carrying capabilities of the laminate.

4. Matrix properties

Intralaminar Mode-II fracture is mainly a test of matrix shearing capabilities as crack extending from notch tip will follow a preferred path in matrix region in between fiber layers. As the samples tested are from different sources, it is difficult to neglect the possibility of different epoxy hardener mix used in both the samples. This variation in matrix properties in samples can be a contributing factor to a slightly lower Mode-II fracture toughness values of fiberglass laminates.

5. Material model

Lastly, these results are based on linear elastic material behavior whereas composites exhibit time dependent viscoelasticity in steady state loading conditions. Viscoelastic nature will allow stress relaxations and give a fracture toughness parameter higher than that obtained using a linear elastic material response. Although, the peak load (P_Q) value obtained from experiments is independent of material model used but the fracture toughness parameter is highly influenced by the assumption of material characteristics. Therefore, fracture toughness results obtained in this project may be underestimated.

B. Discussion on dynamic fracture initiation toughness

1. Sharp crack tip

All the finite element analysis is performed on specimen modeled with a pre-existing notch having a sharp tip. It is not possible to introduce perfectly sharp crack tips with available machining methods and so a 0.5mm slit with rounded tip is cut in the specimen. One way commonly used to produce a sharp crack is to extend the pre-crack by cyclic loading. This method of fatigue pre-cracking is out of scope of this project as fatigue process will induce composite material degradation which would need further understanding of microscopic phenomena occurring within the material before studying its fracture characteristics.

Sharp crack-tips are assumed for simplification in describing cracks and crack propagation direction in FEA codes but it will provide different values of the parameters observed as a rounded tip will have less stress concentration when compared to a sharp one. Thus it is more likely for a rounded tip to sustain higher loads before initiating to propagate. Therefore, assumption of having a sharp crack-tip should itself overestimate specimen's capability to resist fracture.

2. Fracture toughness parameter

Impact fracture toughness for carbon-epoxy is calculated as $40 \text{ MPa}\sqrt{m}$, fiberglass-epoxy is in the range of 100 to $350 \text{ MPa}\sqrt{m}$. But, using a similar code, values obtained from COD relation and dynamic J-integral approach have a difference of 50% with carbon-epoxy giving a value of $62 \text{ MPa}\sqrt{m}$ and fiberglass-epoxy as 50 to $150 \text{ MPa}\sqrt{m}$. It is surprising to notice huge differences in the two values even though they are outputs obtained from the same simulation. This can be attributed to basic definition of COD as being a strain dependent parameter.

Thus observing COD will take into account only the strains developed at an instant due to stresses near the crack-tip. But for a dynamic case involving propagation of stress waves, there is energy being accumulated that may not contribute to crack flank openings instantaneously. Thus dynamic J-integral being an energy based approach, collects the effect of accumulated energy densities. It also has an advantage of not being evaluated using static relations as is done to calculate stress intensity factor from COD history in many earlier studies [26]. Therefore, dynamic J-integral method will be considered as an alternative approach to determine fracture toughness(J) property of a dynamically loaded material.

3. Interfacial strengths

Fiberglass-epoxy compared to carbon-epoxy samples when tested at almost similar impact velocities exhibit an extra ordinarily high fracture toughness values. This can be attributed to many factors like fiber matrix adhesion properties, fiber stiffness characteristics, fiber volume fraction etc.

A strong interfacial bond between fiber and matrix depends on many factors like fiber surface treatment, exposure to humidity, thermal effects during manufacturing etc [27]. Strong interfacial bonding assures effective stress transfer whereas a weak interface has good impact/fracture resistance as fiber-matrix interface develops cracks before allowing matrix to crack. Carbon fiber prepreg samples used for this project are aerospace grade fibers therefore, are expected to be surface treated to give smooth finish and a good interfacial strength that ensures better load transfer from matrix to fibers as compared to fiberglass epoxy samples. The outcome is that carbon fibers bear all the impact induced tensile stresses transferred from matrix and owing to their high stiffness break

leading to crack propagation .

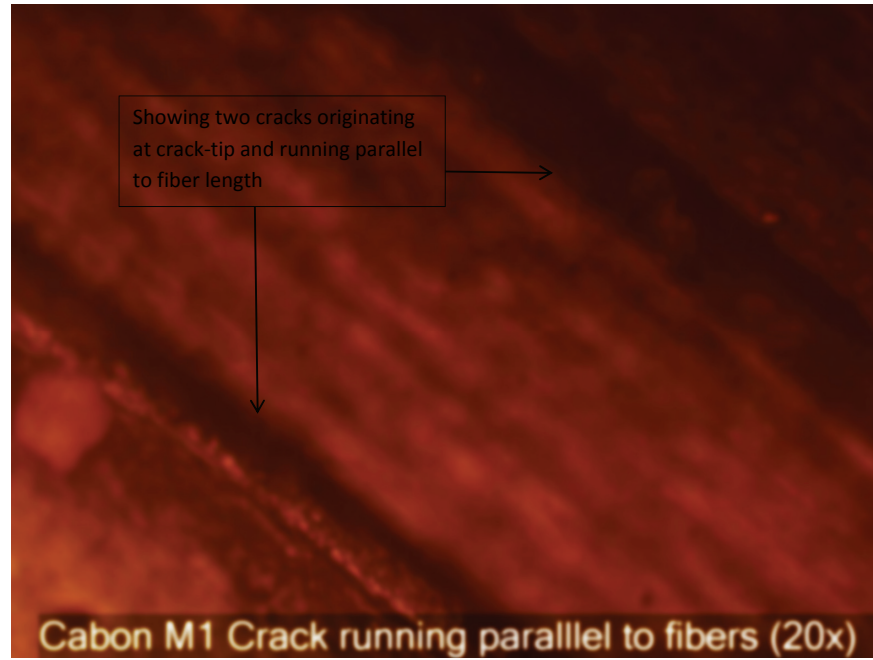
Lower grade hand laid up fiberglass-epoxy having high resin concentrations, the load transfer to fibers is not effective. Moreover, owing to lower interfacial strengths, matrix-fiber interface absorbs most of the stresses and fibers are less strained. Glass fibers having lower stiffness are able to yield relatively easily to give higher resistance to impact forces.

Resin concentrations, interfacial bond characteristics and stress transfer capabilities of both the samples can easily be observed by studying Fig. 29. These microscopic pictures clearly show disturbed interfacial sites in fiberglass epoxy and patterns made in matrix layer between two parallel fibers suggesting, most of the dynamic stresses were absorbed by the interface and matrix layer and load transferred to fibers is not enough to cause failure of the fibers. This theory is also concurrent to visually observed damaged specimens that show no crack propagation to even the next layer of glass fibers whereas carbon-epoxy laminates break into two pieces at the crack plane.

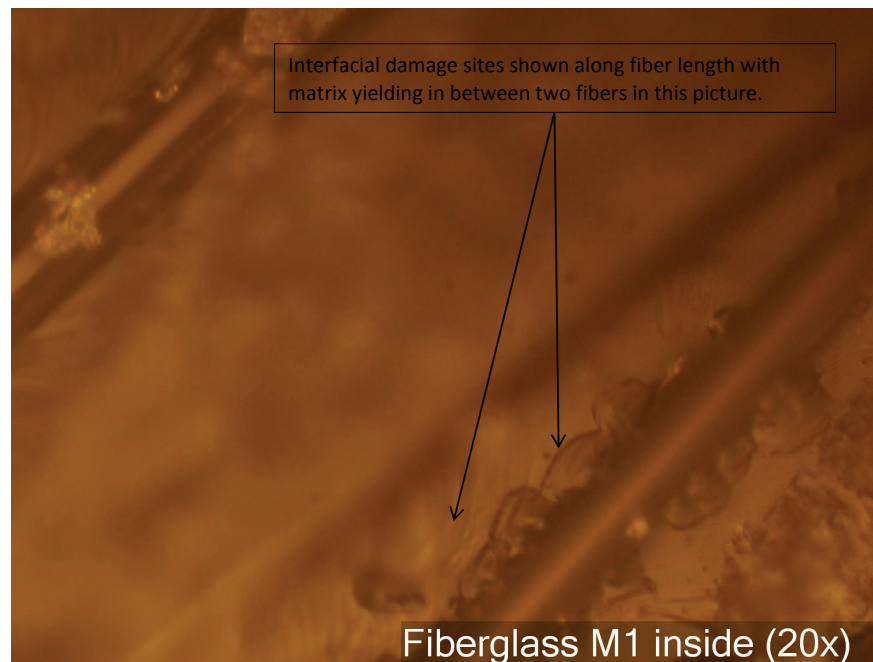
4. Experimental methods

Crack propagation phenomena explained above is relevant for this exercise studying fracture upto point of initiation. The reason being, crack gauge essentially registers the first instant of stresses occurring near the crack tip which will be a slow process in case of fiberglass laminates due to mitigation effects of interfacial failures. Also, this form of damage occurring at interfaces will absorb most of the impact energy rendering sample with lower straining response for the same velocity at impact.

Carbon epoxy samples made of prepregs give consistent values when tested in this project and also when tested by Rubio et al [26]. Owing to good interfacial



(a) Crack in carbon-epoxy laminate(aerospace grade)



(b) Crack in fiberglass-epoxy laminate(lower grade)

Fig. 29. Microscopic pictures comparing interfacial bond characteristics of carbon-epoxy and fiberglass-epoxy samples

properties and immediate stress distribution in the material mass strain gauge responds promptly giving a more precise time instant of around 22 to 27 μsec for crack initiation. Whereas, fiberglass epoxy test output is inconsistent for the samples that are made of lower grade glass fibers through hand lay up process. This may be due to the delay in stress accumulation at the crack gauge on the surface even though the material is continuously being degraded at interfacial sites inside the bulk mass. That is why more than 100 μsec is recorded as time required for crack to initiate in fiberglass samples.

Therefore, it can be inferred that the testing method undertaken may not be most appropriate for such hand laid up materials due to the inconsistent bulk material response.

5. Material properties

To study initiation characteristics of a composite, it is necessary to understand the properties and response of its constituent materials. Even though this project is based on homogeneous composite properties, individual property of each of the constituent plays a role. There are many energy dissipation phenomena that occur in a material before crack actually starts to propagate.

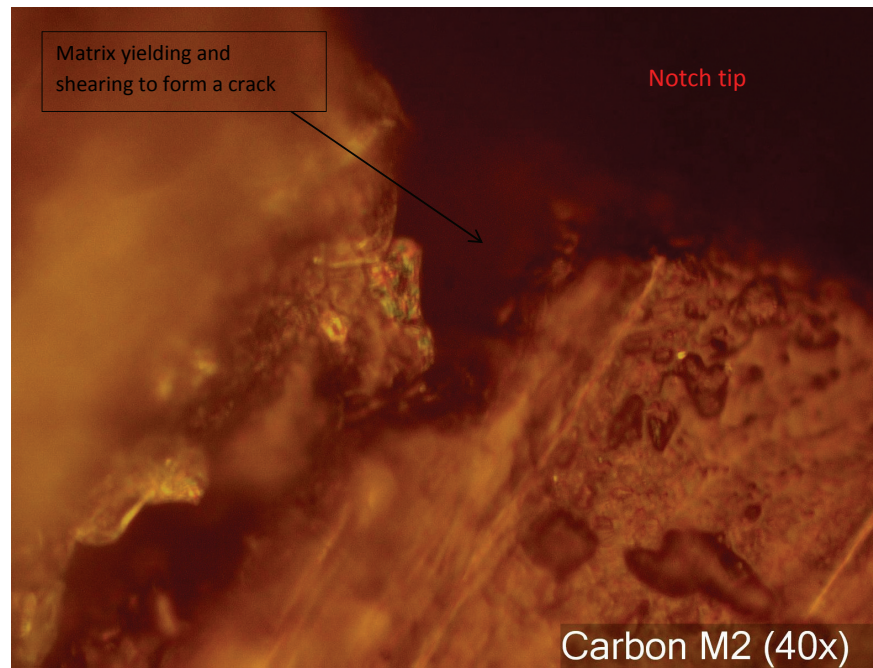
Mode-II fracture toughness results of around $40 \text{ MPa}\sqrt{m}$ and $10 \text{ MPa}\sqrt{m}$ for carbon-epoxy and fiberglass-epoxy is representative of in-plane shear properties of matrix material. Fig. 30 clearly shows matrix shear failure along the fiber lengths. This failure is due to bending leading to compressive stresses on striking half and tensile stresses on supporting half of the specimen. Therefore, in plane shear properties of matrix plays an important role at the instant of crack initiation and later fiber compressive properties decide crack propagation characteristics. This project did not cover the tests for determining the

shear properties but it is generally observed that carbon-epoxy composites have greater in plane shear strengths of around 75 MPa as compared to 40 MPa for fiberglass-epoxy composites [28]. This may be the primary reason for higher strength of carbon-epoxy laminates in Mode-II.

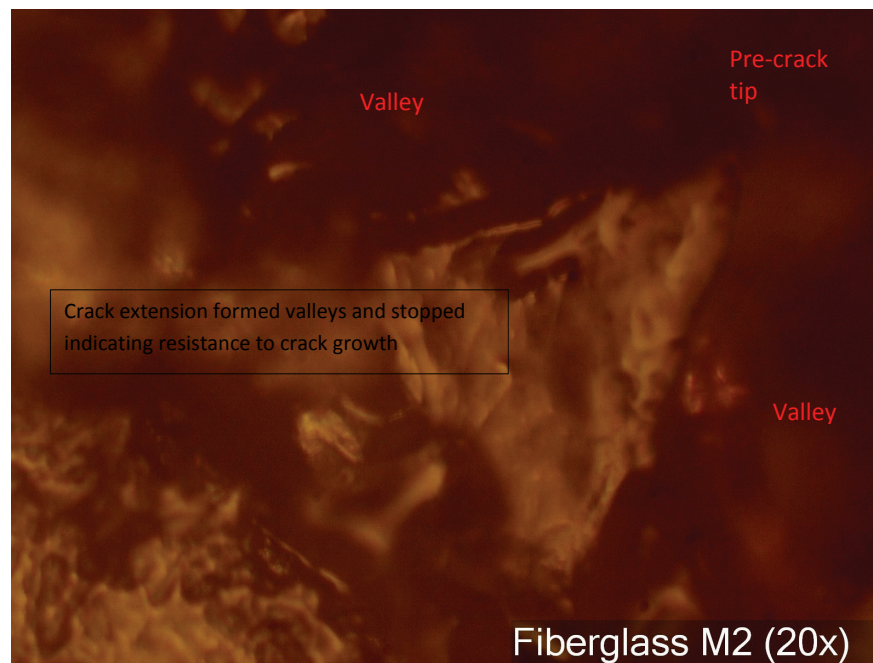
One interesting observation was made during microscopic observation of Mode-II cracks in both composite types. The crack in carbon-epoxy propagated to larger lengths but in fiberglass-epoxy, crack progression stopped very near to crack tip. Some bent glass fibers can be seen at the point where crack stops whereas carbon fibers are entirely broken as shown in Fig. 31. This can be again attributed to effective stress transfer to fibers due to strong interfacial bonding in carbon-epoxy samples leading to brittle failure of fibers under compression. But glass fibers having lower compressive strengths easily yield to absorb impact energy and help in arresting the crack.

6. Non-linear elastic material behavior

Carbon-epoxy samples modeled with non-linear elastic material properties using Hashin damage model in ABAQUS give peculiar results. Referring to Table VI Mode-I dynamic fracture toughness values of around $160 \text{ MPa}\sqrt{m}$ is recorded which is around 2.6 times of values assuming a linear elastic model. This difference in values is quite high to be considered for re-evaluation and further studies on finding a better fitting non-linear model for composite materials. But as explained, composite materials do mitigate the stress concentration effects near the crack tip, by certain non-linear damage phenomena. Thus composite material, even in impact loading conditions does not entirely act as a homogeneous brittle material. Assuming a linear elastic material model will underestimate the material's capability to resist fracture.

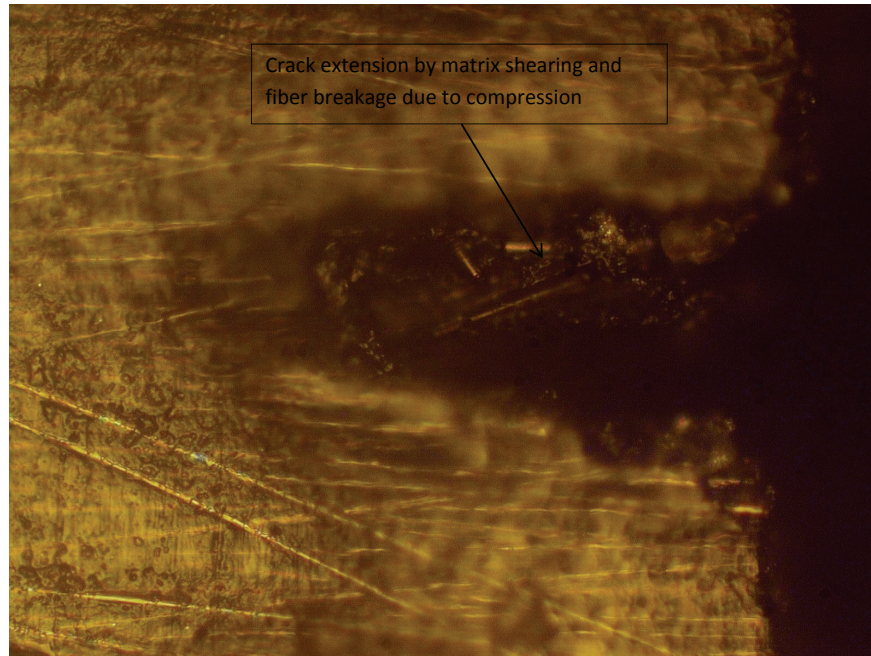


(a) Crack in carbon-epoxy laminate

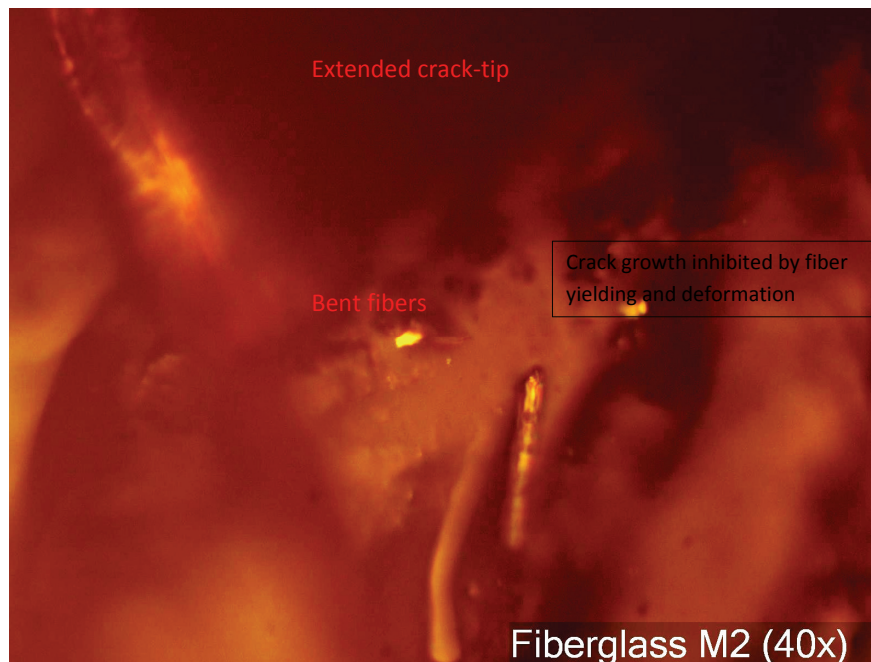


(b) Crack in fiberglass-epoxy laminate

Fig. 30. Pictures from microscope comparing Mode-II in carbon-epoxy and fiberglass-epoxy samples



(a) Crack in carbon-epoxy laminate



(b) Crack in fiberglass-epoxy laminate

Fig. 31. Pictures from microscope comparing Mode-II crack initiation characteristics in carbon-epoxy and fiberglass-epoxy samples

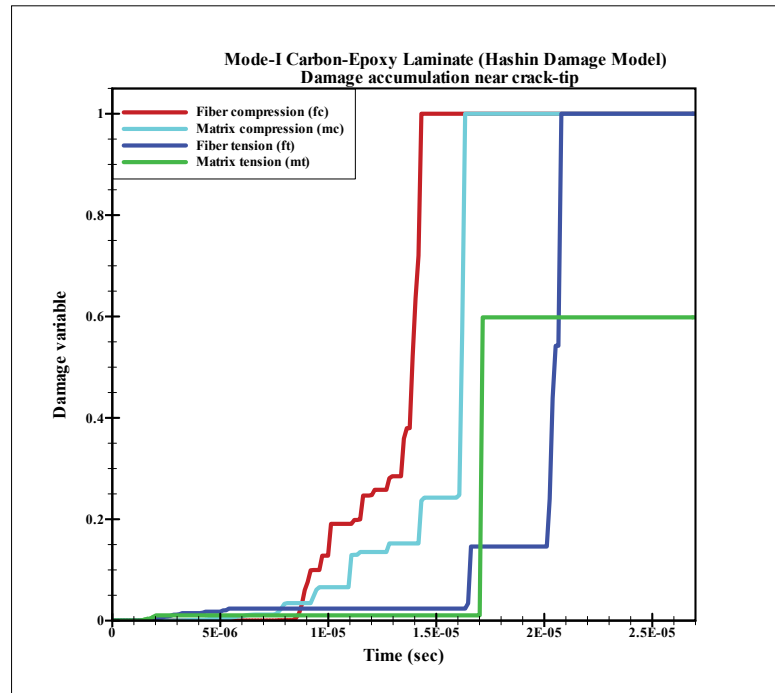


Fig. 32. Study of Mode-I type dynamic crack opening behavior of carbon epoxy laminate

Hashin damage model gives high fracture toughness values may be due to non-existence of important damage variable accounting for interfacial debonding occurring at fiber-matrix interface. Interface debonding is the most prominent mode of material degradation for a Mode-I fracture after which it propagates to break the fibers due tensile stresses transferred by the matrix. The mitigating effects of matrix interfacial failure are ignored resulting in excessive damage energy accumulation prediction by FEA. Fig. 10 shows that crack gauge records compressive stresses near crack-tip as correctly predicted by FEA also in Fig. 32 but it fails to account for interfacial damage. This type of damage will dissipate energy at lower level and thus transfer lesser energy to other damage modes which are on higher energy levels.

For Mode-II, the dynamic fracture toughness value calculated is around 90

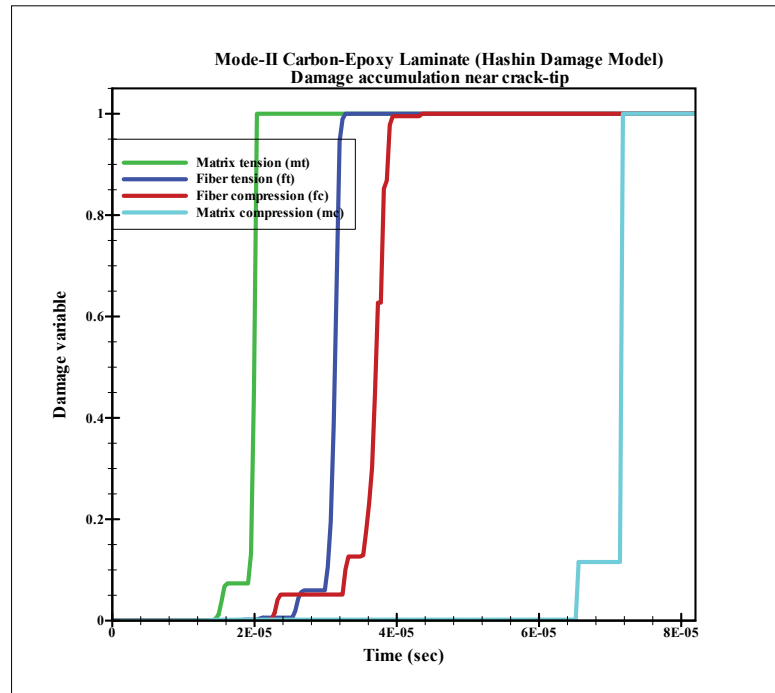


Fig. 33. Study of Mode-II type dynamic crack opening behavior of carbon epoxy laminate

$\text{MPa}\sqrt{m}$ which is around twice the value obtained using a linear elastic model. In this mode of fracture also there is some yielding and then finally shear deformation of the matrix at crack propagation initiation. But it is soon followed by fiber compression thus, energy accumulation, recorded by Hashin model (as shown in Fig. 33), occurs soon after the shear failure actually occurring in experiments. Thus unlike in Mode-I, the gap in real dynamic fracture properties in Mode-II and properties obtained from Hashin damage model should be small.

7. Damage phenomena

Composite laminates are known to exhibit extra ordinary strength characteristics especially in the direction of fibers. Matrix material has the capability to evenly distribute the load to fibers it can be sustained till the ultimate failure point. This is an ideal scenario assuming a perfect composite material. But

manufactured composites contain unavoidable defects like cracks, voids, resin rich zones etc. These flaws are possible sites of stress concentrations and thus are likely to induce damage. Pre-existing flaw is a preferred site for damage accumulation by microcracking to finally result in crack propagation.

Micro-cracks at the crack-tip accumulate to form a macro-crack observed as crack propagation initiation. There occurs a lot of degradation mechanism contributing to formation of these micro cracks depending on the type of loading, boundary conditions, constituents, and their interactions, manufacturing process, environmental degradation etc. The material can be assumed to behave as a homogeneous entity but the results obtained may not be very reliable as these damage mechanisms absorb significant amounts of damage energy before letting the crack tip to evolve.

8. Matted fiberglass fracture toughness

Mat reinforced fiberglass epoxy samples are commonly used in heavy industries. Use of only uni-directional fiberglass plies gives a problem of interlaminar shear. Fiberglass mats are stacked after every three plies of unidirectional fiberglass (20 mils) as this helps in avoiding damage in flexure. The task of testing matted fiberglass epoxy was taken up as an exercise to understand the effects of introducing a discontinuous layer of fiberglass in between uni-directional layers. Referring to Tables.VI and VII dynamic fracture toughness values of around $15 \text{ MPa}\sqrt{m}$ and $3.50 \text{ MPa}\sqrt{m}$ for Mode-I and Mode-II type of fracture clearly suggests that introducing layers of fiberglass mat is detrimental to dynamic fracture toughness properties of a unidirectional laminate. This particular composite type requires careful analysis using a material model to ensure consistent fracture toughness property results.

CHAPTER VII

CONCLUSIONS

Dynamic fracture initiation toughness is an important property needed for reliable component design considerations but there are no standard means to measure material fracture properties at high loading rates. This project introduces a cost effective experimental-numerical approach to calculate dynamic fracture initiation toughness of polymer composites like unidirectional carbon-epoxy and fiberglass-epoxy. Method used provides a step by step procedure starting with impact tests followed by numerical analysis to finally obtain fracture toughness properties of the sample.

High impact velocity tests are conducted in three point bend configuration on SHPB apparatus to obtain dynamic loading history and crack initiation time. Dynamic FEA with a loading boundary condition, as obtained from instrumented impact tests, is then used to obtain relevant parameters required to calculate fracture toughness property of composite material. Mode-I type of fracture test is carried out on SENB specimen geometry and ENF geometry gives Mode-II type of fracture conditions. A quick review of important results obtained are as follows :

- Mode-I dynamic initiation toughness results show a value of $60 \text{ MPa}\sqrt{m}$ for carbon-epoxy which is higher when compared to quasi-tested fracture toughness of $24 \text{ MPa}\sqrt{m}$, indicating that polymer composites have rate dependent properties.
- Dynamic fracture toughness of carbon-epoxy using COD approach gives a value of $40 \text{ MPa}\sqrt{m}$ and dynamic J-integral approach gives $60 \text{ MPa}\sqrt{m}$. Both the approaches are similar but different results are obtained due to a number of assumptions made for their derivations.

- Similarly, Hashin damage model approach has been implemented to account for non-linear phenomena that is expected to occur before actual crack propagation starts. This non-linear elastic damage model in FEA gives a very high value of $150 \text{ MPa}\sqrt{m}$ which needs to be reconsidered.
- Fracture toughness values in Mode-I are observed to be higher than in Mode-II but it is most likely to be a function of fiber alignment with the notch direction.

Proposed methodology gives reliable results when used on consistent carbon-epoxy samples thus providing a sound method to determine dynamic fracture toughness property of polymer composites. This exercise concludes that polymer composites show an improvement in fracture toughness with increase in strain rates. Also, numerical values of fracture properties obtained are observed to be dependent on material properties, fiber layup, manufacturing method, interactions occurring at microscopic level, fracture parameters and material model used to analyze. Thus, while working on this project few key areas could be highlighted for possible improvements and for further work needed to characterize dynamic fracture response of polymer composites.

1. Future work

This project gives an efficient method to study and compare dynamic fracture toughness property of a polymer composite. The methodology involves many assumptions at each step, thus, there is an immense scope of future work. Few of the interesting venues that can be explored further are briefed below:

- The present methodology uses material elastic properties as tested in quasi-static conditions. It will be useful to characterize dynamic response of material and update elastic constants at each time step to obtain more accurate results.

- Dynamic fracture initiation toughness is a material property and thus should not be affected by specimen geometry, crack length etc. Therefore, it will be helpful to conduct validation runs by changing the geometry of the specimen being tested and repeating the impact tests to obtain consistent results each time. This will help in confirming this project methodology aimed at determining fracture toughness property of a material.
- This method is limited by the number of fiberglass epoxy laminates tested due to issues with its repeatability as can be seen from vast differences in results of two good sample tests in Table VI and VII. Therefore, it will be good area to explore the reasons and effects of inconsistent manufacturing processes on dynamic fracture toughness property of a material.
- It will be helpful to develop dynamic relations for calculating time dependent stress intensity factor occurring at discontinuities in a part subjected to dynamic loading conditions. This will eliminate the use of static equations that do not account for time dependent phenomena occurring at stationary crack-tip and thus inducing a possible error in calculating fracture toughness properties of materials.
- It will be beneficial to study the effect of increase or decrease in impact velocity on fracture toughness values and obtaining a trend that can help predict fracture properties of material sample at different loading rates using only the recorded trendline.

REFERENCES

- [1] “Fracture toughness,” Website, Accessed Aug. 27, 2010, <http://www.ndt-ed.org/EducationResources/CommunityCollege/Materials/Mechanical/FractureToughness.htm>.
- [2] J. Fengchun and K. S. Vecchio, “Hopkinson bar loaded fracture experimental technique: A critical review of dynamic fracture toughness tests,” *Applied Mechanics Reviews*, vol. 62, no. 6, pp. 39, Nov 2009.
- [3] K. Friedrich, *Application of Fracture Mechanics to Composite Materials*, vol. 6, Elsevier Science, New York, 1989, 1989.
- [4] E. E. Gdoutos, *Fracture Mechanics: An Introduction, 2nd ed.*, Springer, Norwell, MA, 2005.
- [5] T. Yokoyama and K. Kishida, “A novel impact three-point bend test method for determining dynamic fracture-initiation toughness,” *Experimental Mechanics*, vol. 29, no. 2, pp. 188–194, 1989.
- [6] J. Fengchun, L. Ruitang, Z. Xiaoxin, K. S. Vecchio, and A. Rohatgi, “Evaluation of dynamic fracture toughness K_{id} by Hopkinson pressure bar loaded instrumented charpy impact test,” *Engineering Fracture Mechanics*, vol. 71, no. 3, pp. 279–287, 2004.
- [7] C. Rubio-Gonzalez, J. A. Gallardo-Gonzalez, G. Mesmacque, and U. Sanchez-Santana, “Dynamic fracture toughness of pre-fatigued materials,” *International Journal of Fatigue*, vol. 30, no. 6, pp. 1056–1064, 2008.

- [8] A. Jadhav, “High strain rate properties of polymer matrix composites,” M.S. thesis, Louisiana State University and Agricultural and Mechanical College, Baton Rouge, August 2003.
- [9] J. L. Tsai, C. Guo, and C. T. Sun, “Dynamic delamination fracture toughness in unidirectional polymeric composites,” *Composites Science and Technology*, vol. 61, no. 1, pp. 87–94, 2001.
- [10] “Advances in the simulation of damage and fracture of composite structures,” ABAQUS report by Pedro Ponces Camanho, DEMEGI, Faculdade de Engenharia, Universidade do Porto, Accessed Sept. 01, 2010, <http://www.principia.es/abaqus/abstracts-2005/Abaqus-PPCamanho.pdf>.
- [11] C. Guo and C. T. Sun, “Dynamic Mode-I crack-propagation in a carbon/epoxy composite,” *Composites Science and Technology*, vol. 58, no. 9, pp. 1405–1410, 1997.
- [12] C. T. Sun and C. Han, “A method for testing interlaminar dynamic fracture toughness of polymeric composites,” *Composites Part B-Engineering*, vol. 35, no. 6-8, pp. 647–655, 2004.
- [13] J. Lambros and A. Rosakis, “An experimental study of dynamic delamination of thick fiber reinforced polymeric matrix composites,” *Experimental Mechanics*, vol. 37, no. 3, pp. 360–366, 1997.
- [14] R. M. Davies, “A critical study of the Hopkinson pressure bar,” *Philosophical Transactions of the Royal Society of London Series A Mathematical and Physical Sciences*, vol. 240, no. 821, pp. 375–457, 1948.
- [15] H. Kolsky, “An investigation of the mechanical properties of materials at very

- high rates of loading,” *Proc Phys Soc London Sect B*, vol. 62, no. 2, pp. 676–700, 1949.
- [16] L. S. Costin, J. Duffy, and L. B. Freund, “Fracture initiation in metals under stress wave loading conditions,” *American Society for Testing and Materials*, vol. 627, no. 18, pp. 301–318, 1977.
- [17] J. F. Mandell, S.-S. Wang, and F. J. McGarry, “The extension of crack tip damage zones in fiber reinforced plastic laminates,” *Journal of Composite Materials*, vol. 9, no. 3, pp. 266–287, 1975.
- [18] Y. Mou and R. P. S. Han, “Damage zones based on Dugdale model for materials,” *International Journal of Fracture*, vol. 68, no. 3, pp. 245–259, 1994.
- [19] T. J. Wang, “A continuum damage mechanics criterion for mixed mode ductile fracture,” *International Journal of Fracture*, vol. 63, no. 3, pp. R47–R50, 1993.
- [20] I. Lapczyk and A. J. Hurtado, “Progressive damage modeling in fiber-reinforced materials,” *Composites Part A-Applied Science and Manufacturing*, vol. 38, no. 11, Sp. Iss. SI, pp. 2333–2341, 2007.
- [21] N. E. Merter, “Effects of processing parameters on the mechanical behavior of continuous glass fiber/polypropylene composites,” M.S. thesis, Izmir Institute of Technology, Izmir, Turkey, October 2009.
- [22] M. F. Kanninen and C. H. Popelar, *Advanced Fracture Mechanics, 1st ed.*, Oxford University Press, New York, 1985.
- [23] M. Janssen, J. Zuidema, and R.J.H Wanhill, *Fracture Mechanics, 2nd ed.*, VSSD, The Netherlands, 2006.

- [24] S. T. Lin, Z. Feng, and R. E. Rowlands, “Thermoelastic determination of stress intensity factors in orthotropic composites using the J-integral,” *Engineering Fracture Mechanics*, vol. 56, no. 4, pp. 579–592, 1997.
- [25] C. Rubio-Gonzalez and J. J. Mason, “Dynamic stress intensity factors at the tip of a uniformly loaded semi-infinite crack in an orthotropic material,” *Journal of the Mechanics and Physics of Solids*, vol. 48, no. 5, pp. 899–925, 2000.
- [26] C. Rubio-Gonzalez, J. Wang, J. Martinez, and H. Kaur, “Dynamic fracture toughness of composite materials,” presented at *4th International Conference on Advanced Computational Engineering and Experimenting ACE X 2010*, Paris, France, July 2010.
- [27] H. Zhuang and J. P. Wightman, “The influence of surface properties on carbon fiber/epoxy matrix interfacial adhesion,” *The Journal of Adhesion*, vol. 62, no. 1, pp. 213–245, 1997.
- [28] “Mechanical properties of carbon fibre composite materials, fibre / epoxy resin,” Website, Accessed Sept. 01, 2010, http://www.performance-composites.com/carbonfibre/mechanicalproperties_2.asp.
- [29] SIMULIA, *ABAQUS Manual (Online)*, <http://abaqus.civil.uwa.edu.au:2080/v6.8/> Accessed Aug. 28, 2010.

APPENDIX A

ABAQUS FUNCTIONALITY

Composites exhibit anisotropy and thus their damage onset and evolution is predicted using different theories. Any theory can be implemented to model the degradation of material properties due to stresses induced on loading. The constitutive relation to relate the stresses and strains with the progress of damage at each time step can be defined using UMAT /VUMAT and the criteria for failure in ABAQUS can be used based on maximum stresses, strains, or energy dissipated during damage etc. A damage model requires three inputs for its complete definition:

- Undamaged response: This is basically elastic in nature as the plasticity can be ignored in such materials during initiation. It can be achieved using orthotropic elasticity in plane stress. Or it can be defined by inputting the stiffness matrix directly.
- Damage initiation : A criteria that specifies initiation of damage process.
- Damage evolution : A basis that defines evolution of damage with time in material.

Damage can be characterized as degradation of material stiffness. The models used are basically to compute this stiffness change due to change in damage variables over time because of applied stresses.

ABAQUS has an inbuilt damage model based on Hashin's work. It takes care of four possible modes of failure:

- Fiber failure in tension

- Fiber buckling and kinking in compression
- Matrix cracking due to transverse stresses
- Matrix crushing due to transverse stresses

It uses three internal variables to characterize fiber, matrix and shear damage (in plane stress) derived from four damage variables for all the four failure modes. The updated damage operator gives the effective stress tensor used to evaluate initiation criterion. An output variable associated with initiation criterion will tell if it has been met or not. Damage evolution law uses Hashin's damage initiation criteria and is based on energy dissipated during the damage process.

Once the damage has initiated, to reduce the mesh dependency, characteristic length is introduced for formulation, so that the constitutive law is based on stress-displacement relation. The damage variable is made to evolve in such a way to follow a downward sloping trend of stress vs displacement for each of the failure modes. Various equations used to compute the stresses and damage variables are as follows: The effective stress, σ_{eff} , is degraded as the stiffness degrades because of damage occurring in fibers (d_f) and matrix (d_m). Therefore it is given as

$$\sigma_{eff} = \phi \times \sigma_{nom} \quad (A.1)$$

since anisotropic second order damage tensor is considered, M_{ij}

$$[\sigma_{eff}] = [M] \times [\sigma_{nom}] \quad (A.2)$$

where

$$M = \begin{bmatrix} 1/(1-d_f) & 0 & 0 \\ 0 & 1/(1-d_m) & 0 \\ 0 & 0 & 1/(1-d_s) \end{bmatrix} \quad (\text{A.3})$$

and

$$d_s = 1 - (1-d_{ft})(1-d_{fc})(1-d_{mt})(1-d_{mc}) \quad (\text{A.4})$$

where

d_{ft} : Fiber tensile damage

d_{fc} : Fiber compressive damage

d_{mt} : Matrix tensile damage

d_{mc} : Matrix compressive damage

The stiffness matrix obtained is

$$C = \frac{1}{D} \begin{bmatrix} (1-d_f)E_1 & (1-d_f)(1-d_m)\nu_{12}E_1 & 0 \\ (1-d_f)(1-d_m)\nu_{21}E_2 & (1-d_m)E_2 & 0 \\ 0 & 0 & (1-d_s)GD \end{bmatrix} \quad (\text{A.5})$$

where

$$D = 1 - (1-d_f)(1-d_m)\nu_{12}\nu_{21}$$

d_{ft} , d_{fc} , d_{mt} , d_{mc} are assumed as internal state variables to estimate the damage dissipation function. Thus a material initially being orthotropic in nature will evolve to show anisotropic behavior later due to damage.

Helmoltz free energy is assumed as a function of elastic strains and damage variables (d_{ft} , d_{fc} , d_{mt} , d_{mc}) and the material is assumed to behave elastically under isothermal conditions.

$$\text{Energy} = f(\epsilon, d_{ft}, d_{fc}, d_{mt}, d_{mc}) \quad (\text{A.6})$$

Thermodynamic forces leading to each of these damage modes are computed as

$$Y_1 = \frac{\partial G}{\partial d_1} \quad (\text{A.7})$$

Gibbs free energy,

$$G = \frac{1}{2E_1} \left(\frac{\langle \sigma_{11} \rangle^2}{(1-d_{ft})} + \frac{\langle -\sigma_{11} \rangle^2}{(1-d_{fc})} \right) + \left(\frac{\langle \sigma_{22} \rangle^2}{(1-d_{mt})} + \frac{\langle -\sigma_{22} \rangle^2}{(1-d_{mc})} \right) - \frac{\nu_{12}\sigma_{11}\sigma_{12}}{E_1} + \frac{\sigma_{12}^2}{(1-d_s)G_{12}} \quad (\text{A.8})$$

Damage dissipation energy is then given as,

$$\dot{G} = Y_{ft}\dot{d}_{ft} + Y_{fc}\dot{d}_{fc} + Y_{mt}\dot{d}_{mt} + Y_{mc}\dot{d}_{mc} \quad (\text{A.9})$$

The following criterions have been used to study various stages of damage:

Initiation of damage

Method to predict the initiation of damage is based on Hashin's model that describes four possible modes of failure in unidirectional composites. It is based on the effective stress components computed with the help of above relations

$$\text{Fibertension}(\hat{\sigma}_{11} \geq 0); F_{ft} = \left(\frac{\hat{\sigma}_{11}}{X^T} \right)^2 + \alpha \left(\frac{\hat{\sigma}_{12}}{S^L} \right)^2 \quad (\text{A.10})$$

$$\text{Fibercompression}(\hat{\sigma}_{11} < 0); F_{fc} = \left(\frac{\hat{\sigma}_{11}}{X^C} \right)^2 \quad (\text{A.11})$$

$$\text{Matrixtension}(\hat{\sigma}_{22} \geq 0); F_{mt} = \left(\frac{\hat{\sigma}_{22}}{Y^T} \right)^2 + \left(\frac{\hat{\tau}_{12}}{S^L} \right)^2 \quad (\text{A.12})$$

$$\text{Matrixcompression}(\hat{\sigma}_{22} < 0); F_{fc} = \left(\frac{\hat{\sigma}_{22}}{2S^T} \right)^2 + \left[\left(\frac{Y^C}{2S^T} \right)^2 - 1 \right] \frac{\hat{\sigma}_{22}}{Y^C} + \left(\frac{\hat{\tau}_{12}}{S^L} \right)^2 \quad (\text{A.13})$$

where

$\hat{\sigma}_{ij}$ are the components of the effective stress tensor σ_{eff}

X_T and X_C are Tensile & Compressive strengths in fiber Direction

Y_T and Y_C are Tensile & Compressive strengths in matrix Direction

S_L and S_T are longitudinal and transverse shear strength

Evolution of damage

Once damage is initiated, the stiffness $[C]$ degrades as shown in above relations and damage evolves as per damage law based on the fracture energy dissipated in each of the failure modes. If it meets the critical values defined, the damage further propagates[20, 29].

APPENDIX B

MATLAB CODE FOR SHPB SIGNAL PROCESSING AND STRESS
INTENSITY FACTOR CALCULATIONS

```

1  % Prueba. Hopkinson bar, three point bending test signal
   processing.
2
3  clear all
4  close all
5  clc
6  d=19; %bar diameter mm
7  E=190e9; %Young's modulus (MPa)
8  A=pi*(d^2)/4; %Bar area
9
10 load pulso1.txt %Incident bar pulse
11 load pulso3.txt % Crack strain gauge signal
12
13 p1=pulso1;
14 t1=p1(:,1);
15 v1=p1(:,2);
16 vm=mean(v1(2:10)); %reference to zero the signal
17 v1=v1-vm;
18
19
20 p3=pulso3;
21 t3=p3(:,1);
22 v3=p3(:,2);
23 vm3=mean(v3(2:10));
24 v3=v3-vm3;
25
26
27
28 f=fspecial('gauss',[25 1],5);
29 vf1=conv(v1,f,'same');%filter(f,1,v1);
30 correccion=7;
31
32 figure(1)
33 plot(t1,v1,t1,vf1)
34 xlabel('time (s)')
35 ylabel('voltage')
36 title('Filttered and unfilttered original signals')
37
38 grid
39
40 Sg=2.095; %gage factor
41 GIR=1000; %gain incident and reflected pulse

```

```

42 GTS=5000; %gain transmitted pulses
43 VEIR=3.5; %voltage incident and reflected pulse
44 VETS=7; %voltage transmitted pulses
45
46 SgP=2.13; % gage factor strain gage at the specimen
47 GP=200; % gain at the specimen
48 VP=3.5; %voltage at the specimen
49
50
51 e1=(vf1*4)/(VEIR*GIR*Sg);
52
53 ep=(v3*4)/(VP*GP*SgP);
54
55 t11=t1(1);
56 figure(2)
57 plot((t1-t11)*1e6,e1,(t3-t11)*1e6,ep)
58 xlabel('time (\mu s)')
59 ylabel('strain')
60 grid
61
62 i=4;
63 periodo=375;
64 diferencias=zeros(fix(periodo/8),1);
65 for j=0:periodo/8
66     diferencias(j+1)=abs(e1(i+j)+e1(i+370+j));
67 end
68 [error,p]=min(diferencias);
69 nn1=(p-1)+i;
70 nn2=nn1+375;
71 nt=length(t1);
72 ti=t1(nn1:nn1+100)-t1(nn1);
73 tr=t1(nn2:nn2+100)-t1(nn2);
74
75
76 ei=e1(nn1:nn1+100);
77 er=e1(nn2:nn2+100);%-e1(nn2);
78 eir=ei+er;
79
80 mi=(ei(end)-ei(1))/size(ti,1);
81 r_i=mi*(0:size(ti,1)-1)+e1(nn1);
82
83 mr=(er(end)-er(1))/size(tr,1);
84 r_r=mr*(0:size(tr,1)-1)+e1(nn2);
85 ei=ei-r_i;
86 er=er-r_r;
87 eir=ei+er;
88
89
90 figure(3)
91 plot(ti*1e6,-ei,':',tr*1e6,er,'--',tr*1e6,eir)
92 xlabel('time (\mu s)')

```

```
93 ylabel('strain')
94 legend('incident','reflected','resultant')
95 title('Sum of incident and reflected pulses')
96 grid
97
98
99 %—— forces
100 f1=E*A*1e-9*eir; %incident force
101
102 figure(5)
103 plot(tr*1e6,f1)
104 xlabel('time (\mu s)')
105 ylabel('force (kN)')
106 title('dynamic load')
107 axis([0,100,-60,20])
108 grid
109
110 temp=[tr,-ei,er,eir];
111 xlswrite('wave.xls',temp)
```



```

1 % Stress intensity factor calculation using COD
2 clear
3 % Carbon
4 Ex=8.1e9;
5 Ey=107.7e9;
6 Ez=8.1e9;
7 Gxy=3.85e9;
8 Gxz=3.85e9;
9 Gyz=3.85e9;
10 nuxy=.025;
11 nuxz=.34;
12 nuyz=.34;
13 rho=1505.8;
14
15 %plane stress
16 a11=1/Ex;
17 a22=1/Ey;
18 a12=-nuxy/Ex;
19 a66=1/Gxy;
20
21 a=a11;b=2*a12+a66;c=a22;
22 mul1s=(-b+sqrt(b^2-4*a*c))/(2*a);
23 mu2s=(-b-sqrt(b^2-4*a*c))/(2*a);
24 w1=sqrt(-mul1s)
25 w2=sqrt(-mu2s)
26
27 c11=Ex/(Gxy*(1-(Ey/Ex)*nuxy^2))
28 c22=(Ey/Ex)*c11
29 c12=nuxy*c22
30
31 cs=sqrt(Gxy/rho)
32 cd=sqrt(c11)*cs
33
34 % COD at r=1mm
35 load u2_c12_n20.txt
36 t=u2_c12_n20(:,1);
37 v=u2_c12_n20(:,2);
38
39 load load_hist_c12.txt % load history
40 t1=load_hist_c12(:,1);
41 p1=load_hist_c12(:,2);
42
43 r=.001; % Distance of strain gauge from crack tip
44
45 % Stress intensity factor
46 K=v/1000*(pi*w1*w2/(sqrt(2*pi*r)*(w1+w2)*a22));
47 figure(1)
48 plot(t*1e6,v*1e3)
49 xlabel('time (\mus)')
50 ylabel('Vertical displacement (mm)')

```

```
51 grid
52
53 t=t*1e6; K=K*1e-6;
54 figure(2)
55 plot(t,K)
56 xlabel('time (\mus)')
57 ylabel('Stress Intensity Factor (MPa(m)^{1/2})')
58 grid
59 title('SIF history')
60
61 figure(3)
62 plot(t1*1e6,p1*1e-3)
63 xlabel('time (\mus)')
64 ylabel('Load (kN)')
65 grid
66 title('Load history')
```

VITA

Name Harmeet Kaur

Address Sector-C, Pocket-2, H.No:2125
 Vasant Kunj, New Delhi-70

Email Id mann.harmeet@gmail.com

Education B.E. Mechanical, Rajasthan Univerity, Kota, India
 M.S. Mechanical Engineering, Texas A&M University,
 College Station, USA